Response to the Editor

Dear Dr. Hrachowitz,

Thank you for evaluating our manuscript and review responses with a keen eye and providing constructive comments. We have modified our manuscript to address all review comments. In particular, we have significantly expanded the discussion of the method used in the manuscript, paying special attention to comments from Reviewer 1 (see Section 3.2.1). It is hoped that this will serve as a self-contained explanation of the method. We have also provided additional discussion on DA methods so as to explain the reasons for adopting an EnKF based approach (see Lines 233-241) along with its main limitation (i.e. the sub-optimal update, see Line 236).

We have also modified the introduction so that the science questions of interest are more clearly stated (see Lines 89-113). These are two specific issues that arise when applying the time varying parameter method to realistic study settings, which, to the best of our knowledge, has not been previously investigated. We summarise our approach to investigating these issues in Lines 115-127. More details of the practical applications of the time varying method have also been provided, as requested by Reviewer 2 (see Lines 33-40, 75-84).

In regards to the comment on separating meteorological and land use change contributions: we acknowledge that the interpretations from our analysis were oversimplified in our initial response. Our intent is to demonstrate that the time varying parameter approach can be used to show that observed changes to streamflow are not solely a result of changes in the meteorological patterns (as per the analysis at the end of Section 4). We have provided additional discussion to make clear how the analysis should be interpreted, taking into consideration helpful comments from both Reviewer 2 and the Editor (see Lines 479-484, 482-484). Specifically, it cannot be used to precisely separate out the contributions of forcing and land use change; the analysis can only be used to show that either 1) meteorological changes are the main driver of streamflow changes or 2) land cover changes are contributing to hydrologic change (but potentially in addition to meteorological changes due to the presence of ecosystem feedbacks, as noted by the Editor).

Full details of our revisions can be found in the response to reviewer documents, along with responses to all comments.

Thank you for your time and consideration.

Best Regards,

Sahani Pathiraja
Daniela Anghileri
Paolo Burlando
Ashish Sharma
Lucy Marshall
Hamid Moradkhani

Response to reviewer 1

Please note all line references refer to the revised document with tracked changes.

The authors are performing data assimilation (DA), for a dynamical hydrological model with time-varying parameters. I fully agree that, in hydrology, time-varying parameters very often lead to a more realistic description of reality than constant ones, with the caveat that a good stochastic model for their dynamics is used. That being said, I have serious doubts about the validity of the method used in this paper.

We thank the reviewer for their time. Please see below our responses to specific comments.

First of all, there is no clear separation between the hydrological model assumptions and the numerical method that is used for DA. The model assumptions should not only comprise the deterministic hydrological equations and the observational error assumptions, but here also a precise definition of the assumed stochastic dynamics of the model parameters. These assumptions have nothing to do with DA, but are part of our prior knowledge about the system. Together with prior probability distributions, e.g. for initial conditions, and measured data they completely define the posterior as well as predictive distributions of states and parameters.

We have provided additional explanation on how the prior parameters are generated in the revised manuscript (see Lines 268-286). This is undertaken in Step 1 of the algorithm in Section 3.2.1. The assumed parameter dynamics are a Gaussian random walk with time varying mean and variance. This is a reasonable assumption for cases where no prior knowledge of the parameter dynamics (or changes to catchment properties) is available. The prior mean is assumed to evolve locally linearly in time, such that it is estimated by the drift rate from the previous two time steps (eqn 1 and eqns 3-5). The prior variance is assumed to be also time dependent, and based on the variance at the previous time (eqn 2). The statistics of the prior parameter ensemble are updated sequentially by the DA algorithm based on assimilated observations.

We have also provided more detailed explanations of the other steps in the algorithm (see Section 3.2.1). It is hoped that this will serve as a self-contained explanation of the method.

All DA methods must lead to the same distributions and the choice is only a matter of computational efficiency. If this separation is not clearly made, there is a risk that inference (here DA) and prediction is done under different model assumptions, which would be inconsistent and lead to a loss of interpretability of the results. I've been trying to do this separation and unveil the assumptions behind the dynamics of the parameters from step 1 of the numerical DA algorithm, but it is not obvious to me what these assumptions are. Without constraining data (i.e. in a predictive mode), what would be the dynamics of the parameter distribution?

We have provided additional discussion to make clear the DA method used, associated limitations, and why it has been adopted (see Lines 233-243). DA methods in general do not lead to the same posterior distributions, particularly when applied to complex non-linear/non-Gaussian problems. This is even when one is specifying the prior, initial conditions and observation error in exactly the same way. For instance, Kalman Filter based methods (e.g. Ensemble Kalman Filter, Ensemble Transform Kalman Filter, Ensemble Adjustment Kalman Filter) consider only the mean and covariance in generating the update (see Line 236), whilst Particle Filter methods (e.g. Particle Filter-SIR, Particle Filter-MCMC, Auxiliary Particle Filter) aim to propagate the full probability density through time (see Line 239-240). They do not differ solely in terms of computational efficiency (e.g. Arulampalam et al., 2002; Liu et al., 2007). An

EnKF based approach has been adopted because it is a practical alternative to Particle Filter/Sequential Monte Carlo methods with demonstrated success in many hydrologic applications (see Lines 237-239).

The assumed parameter stochastic dynamics were discussed in the response to the previous comment; these apply in predictive/forecast mode also. In this case, the proposed local linear extrapolation is only valid close to the current time point. This is acceptable given that the Locally Linear Dual EnKF is designed for short term predictive modelling/forecasting. This has been made clear in Lines 327-332. The intended use of the algorithm has also been explicitly described in Lines 75-81.

Putting aside my concerns about these model assumptions, I have even more serious concerns about the chosen DA method, which seems to violate the assumptions behind Kalman filters in at least two ways:

(i) Kalman filters assume normality of the distribution of the augmented state (incl. parameters). Is there any reason to believe that the non-linearity of the chosen hydrological model is weak enough for this assumption to be approximately valid? Given the dimensionality of the model and the data, respectively, I'm almost certain that it will be grossly violated.

We note that the method relies on an Ensemble Kalman Filter, not a standard Kalman Filter. Ensemble Kalman Filters were specifically designed to handle the non-linear/non-Gaussian case. This means that they at least partially consider non-Gaussianity in state variables, as the full non-linearity of the forward model is considered when calculating prior variables. However, they are sub-optimal in that only the mean and covariance are considered in calculating the update or posterior. Nevertheless, they are a practical alternative to Sequential Monte Carlo methods (which approximate the full Bayesian posterior), as these methods suffer from several practical implementation issues even in moderate dimensional problems (such as degeneracy and sample impoverishment). We also note that Ensemble Kalman Filters have been used with considerable success in a wide range of complex non-linear/non-Gaussian problems (see for Reichle et al., 2002; Gu et al., 2005; Komma et al., 2008; Sun et al., 2009; Xu et al., 2016).

We have provided further discussion in the manuscript in relation to the above (please see lines 232-243).

(ii) Updating the states, based on prior predictions that have been made with parameters that have already been updated seems to use the data twice. This again seems to violate model assumptions, or in other words, I have no idea what the model assumptions are, for which the proposed method is a valid DA.

Please note that in Step 6 of the algorithm (Section 3.2.1), the Kalman Update equation for correlated process and measurement noise is used instead of the standard Kalman update equation. This is used precisely to account for the fact that the observations have already been used in generating the prior states. A detailed derivation of these equations (i.e. equations 15 to 18 in the revised manuscript) can be found in the Appendix B of Pathiraja et al. (2016). We have provided additional words in the revised manuscript to emphasise this point (see lines 314-318).

References

Arulampalam, M. S., S. Maskell, N. Gordon, and T. Clapp (2002), A tutorial on particle filters for online nonlinear/non-Gaussian Bayesian tracking, *IEEE Trans. Signal Process.*, *50*(2), 174–188, doi:10.1109/78.978374.

Gu, Y., and D. S. Oliver (2005), History matching of the PUNQ-S3 reservoir model using the ensemble Kalman filter, *SPE J.*, *10*(2), 217–224, doi:10.2118/89942-PA.

Komma, J., G. Blöschl, and C. Reszler (2008), Soil moisture updating by Ensemble Kalman Filtering in real-time flood forecasting, *J. Hydrol.*, *357*(3–4), 228–242, doi:10.1016/j.jhydrol.2008.05.020.

Liu, Y., and H. V. Gupta (2007), Uncertainty in hydrologic modeling: Toward an integrated data assimilation framework, *Water Resour. Res.*, *43*(7), doi:10.1029/2006WR005756.

Pathiraja, S., L. Marshall, A. Sharma, and H. Moradkhani (2016), Hydrologic modeling in dynamic catchments: A data assimilation approach, *Water Resour. Res.*, *52*, 3350–3372, doi:10.1002/2015WR017192.

Reichle, R. H., D. B. McLaughlin, and D. Entekhabi (2002), Hydrologic Data Assimilation with the Ensemble Kalman Filter, *Am. Meteorol. Soc. - Mon. Weather Rev.*, *130*(1), 103–114, doi:10.1175/1520-0493(2002)130<0103:HDAWTE>2.0.CO;2.

Sun, A. Y., A. Morris, and S. Mohanty (2009), Comparison of deterministic ensemble Kalman filters for assimilating hydrogeological data, *Adv. Water Resour.*, *32*(2), 280–292, doi:10.1016/j.advwatres.2008.11.006.

Xu, T., and J. . Gomez-Hernandez (2016), Joint identification of contaminant source location, initial release time, and initial solute concentration in an aquifer via ensemble kalman filtering, *Water Resour. Res.*, 600–612, doi:10.1002/2015WR018249.

Response to reviewer 2

Please note all line references refer to the revised document with tracked changes.

This manuscript tested a time varying model parameter framework at a river basin under significant land cover changes in the last few decades. The employed framework is based on Locally Linear Dual EnKF proposed by the authors in the previous studies and is applied to the two conceptual hydrologic models (i.e. HBV and HyMOD).

The manuscript shows interesting result and well written in general. However, I have concerns regarding practical applications of the tested approach and the objectives of this research from the following aspects.

We thank the reviewer for their time and overall positive assessment of the manuscript. We are also grateful for the constructive comments to make clear the contributions of our work. Please see below responses to specific comments.

1. In the abstract, the authors stated "rapid land use change impacts on catchment hydrology" and "therefore modeling methodology of such change is important" in the first and second sentences. First of all, please clarify "for what purpose" such modelling representing the land cover change is thought to be needed. This could be, for example, estimating future water resources under further land cover and climate changes or identifying the physical mechanisms of the impact of land cover change on hydrology. Please explain in the introduction for what objective the authors think the modeling with time varying parameter is necessary.

We appreciate the reviewer's comments that highlight the need to more clearly state the objectives/potential applications of the time varying parameter modelling method. We have provided additional discussion to ensure this is made clear. One of the main purposes is to propose a modelling methodology that can provide accurate predictions even when the catchment conditions are changing in real time, as traditional modelling methods are poorly suited to this task (see Lines 33-35 and 55-57). This is useful for forecasting purposes (e.g. flood forecasting) and also for real time reservoir operation in water resource management (see Lines 35-40 and 75-81). It can also be used to retrospectively assess how model parameters vary in time as a result of land cover changes (see Line 78).

2. Based on the firs point, please explain how the applied framework with the EnKF can achieve the objectives. Obviously the presented approach requires a full set of input and output to estimate the parameter changes. Suppose that this approach now successfully estimates the time-varying parameters in the HBV model, how can this information be useful for water management, given already land cover change has happened and streamflow change has been already detected in the actual catchment.

As discussed above, the Locally Linear Dual EnKF can be useful for retrospective analysis of variations to model parameters and also for predictive purposes. From a prediction perspective, the framework is useful for short term predictions of hydrologic variables in catchments that are undergoing change, where no knowledge of the change is available. The reason it can be used in this context is because parameters are being updated on-the-fly, at

the observation time scale (see Lines 64-66, 73-75). In other words, states and parameters are sequentially changed in real time, whenever an observation becomes available. The most recent observations are then used to make short term predictions of states and parameters (Steps 1-3 in Section 3.2.1). We have provided additional discussion to help clarify how the Locally Linear Dual EnKF can be used for prediction (see Lines 81-82 and 328-332).

3. Related to the above point, please state clearly the main objective of this research in the introduction. Is the main objective here to test the time varying model parameter framework in the data limited catchment? In such case, what is the criteria to conclude the objective has been achieved. The EnKF may show the parameter changes, but is it enough to validate the method? Or is the main objective here to compare the two model structures?

The main objectives of this research are two-fold:

1) To investigate the efficacy of the time varying parameter method in a medium sized catchment with realistic land cover change. This goes beyond previous work which focused on small experimental catchments that had drastic land use changes that are easier to infer from streamflow, and are not representative of realistic studies; and
2) To highlight the importance of the chosen model structure in ensuring the success of the time varying parameter method.

We have modified the introduction so that these objectives are explicitly stated (see Lines 89 - 113), along with providing more discussion on the second issue relating to model structure selection (see in particular Lines 109-113).

In regards to validation of the time varying parameter method, its efficacy was assessed based on the ability to represent all aspects of the streamflow hydrograph. In Section 4, we showed that time varying parameter HBV model provided a good representation of baseflow, total and direct runoff (see Figure 7 and 8, and discussion in Lines 445-469). We also showed that the time varying parameter HyMOD model did not represent all aspects of the hydrograph. This showed the importance of the chosen model structure in determining the success of the time varying parameter method.

With the above main review comments, I have the followings minor comments.

1. Abstract L18 and L57: "it serves as an effective tool for separating the influence of climatic and land use change": is this really true? As a result of the EnKF, it is possible that the both effects of land cover and climate changes may be reflected in the wrong way. Given such an ill-identified potential, please explain the logic and actual steps to distinguish the impacts of the two changes.

We acknowledge that the wording in the abstract is misleading and does not accurately describe the utility of the analysis in Section 4. Our intent is to demonstrate that the time varying parameter approach can be used to show that observed changes to streamflow are not solely a result of changes in meteorological patterns. This is in reference to the analysis undertaken in Section 4 where a resampled rainfall and temperature time series was used with the time varying parameter HBV model (see Lines 471-494). It was found that the

resulting simulated streamflow largely reproduced the changes in the observed streamflow (see Lines 486-487 and Figure 8d and h), thereby lending further weight to the conclusion that land cover change has impacted catchment hydrology. This is intended to also demonstrate that the parameter changes correspond to actual changes in catchment hydrology, and are not simply random changes that happen to reproduce the observed streamflow only when the observed forcing time series is used (this discussion has now been inserted into the manuscript, see Lines 492-494).

We have modified the abstract, introduction and conclusion so that the intended message is clearer (see Lines 17-21, 66-70, 504- 507). We have also provided additional discussion explaining the range of plausible conclusions from our analysis, based on the helpful comments from both Reviewer 2 and the Editor (see Lines 479-484). Specifically, it cannot be used to precisely separate out the contributions of forcing and land use change; the analysis can only be used to show that either 1) meteorological changes are the main driver of streamflow changes or 2) land cover changes are contributing to hydrologic change (but potentially in addition to meteorological changes due to the presence of ecosystem feedbacks, as noted by the Editor).

2. P7 L122 Subsection of "2.1 " may be eliminated because no "2.2" exists.

An additional sub-heading: “2.1 Data & Land Cover Change” has been inserted to separate the different topics of discussion. The previous Section 2.1 subheading is now Section 2.2.

3. P10 L206 Is the covariance matrix (sigma) also updated in the sequential Kalman Filter algorithm? Please clarify this part and show the equation if it is also updated.

The term $\boldsymbol{\Sigma}_{t-1}^{\theta}$ is the sample covariance of the updated (or posterior) parameter ensemble $\left\{\boldsymbol{\theta}_{t-1}^{i+}\right\}_{i=1:n}$ at time *t-1*. In Ensemble Kalman Filtering, the covariance matrix is not explicitly updated, but is replaced by the sample covariance of the updated parameter/state members. The equation for updating the members is given in equations 1 and 3 of the original manuscript.

An equation defining $\boldsymbol{\Sigma}_{t-1}^{\theta}$ has been provided (see equation 2 in revised manuscript).

4. P10 L218 The same comment is also applied to the Kalman gain of the model parameters.

We assumed this comment is in reference to the sample covariance matrices used to calculate the Kalman gain. Similarly, we have provided equations specifying how these covariance matrices are calculated (see equations 11 and 12 in revised manuscript) and emphasised that it is the sample covariance (see e.g. line 304).

5. P12 L261 How did you select the tuning parameter s2? The used values in this manuscript should be shown. Table 4 shows "Initial s2 (VVM)" which confuses me because I thought that s2 were set as constant value for each parameter.

We have expanded the discussion on how the s^2 was tuned. In the original submission, we indicated that it was tuned based on the log score of forecast streamflow. We have expanded

this discussion to provide more details on this, including equations (see Lines 356-363). The values adopted are shown in Table 4, and are constant values. The column header in Table 4 has been changed to just "s^2." We apologise for the error here.

6. P17 "a MASH undertaken..." Please add a brief explanation of the MASH approach.

We have provided more details of the MASH approach (see Lines 187 – 189): "The MASH tool can be used to qualitatively assess interannual variations in the seasonal pattern of a variable. It works by calculating a statistic of the data (e.g. mean) over the same block of days in consecutive years."

Time varying parameter models for catchments with land use change: the importance of model structure

S. Pathiraja[1], D.Anghileri[2], P. Burlando[2], A. Sharma[1], L. Marshall[1], H. Moradkhani[3]

[1]Water Research Centre

School of Civil and Environmental Engineering

University of New South Wales

Sydney, NSW

AUSTRALIA

Email: s.pathiraja@unsw.edu.au

[2]Institute of Environmental Engineering

ETH Zurich

Zurich

SWITZERLAND

[3]Department of Civil and Environmental Engineering

Portland State University

Portland, Oregon

USA

Abstract

Rapid population and economic growth in South-East-Asia has been accompanied by extensive land use change with consequent impacts on catchment hydrology. Modelling methodologies capable of handling changing land use conditions are therefore becoming ever more important, and are receiving increasing attention from hydrologists. A recently developed Data Assimilation based framework that allows model parameters to vary through time in response to signals of change in observations is considered for a medium sized catchment (2880 km^2) in Northern Vietnam experiencing substantial but gradual land cover change. We investigate the efficacy of the method as well as the importance of the chosen model structure in ensuring the success of time varying parameter methods. The framework was utilized with two conceptual models (HBV and HyMOD) that gave good quality streamflow predictions during pre-change conditions. Although both time varying parameter models gave improved streamflow predictions under changed conditions compared to the time invariant parameter model, persistent biases for low flows were apparent in the HyMOD case. It was found that HyMOD was not suited to representing the modified baseflow conditions, resulting in extreme and unrealistic time varying parameter estimates. This work shows that the chosen model can be critical for ensuring the time varying parameter framework successfully models streamflow under changinged land cover conditions. It can also be used to ~~also serves as an effective tool for~~determine whether land cover changes (and not just meteorological factors) contribute to the observed hydrologic changes ~~separating the influence of climatic and land use change~~ in retrospective studies where the lack of a paired control catchment precludes such an assessment.

1. Introduction

Population and economic growth in South-East Asia has led to significant land use change, with rapid deforestation occurring largely for agricultural purposes [*Kummer and Turner*, 1994]. Forest cover in the Greater Mekong Sub-region (comprising Myanmar, Thailand, Cambodia, Laos, Vietnam, and South China) has decreased from about 73% in 1973 to about 51% in 2009 [*WWF*, 2013]. Vietnam in particular has had the second highest rate of deforestation of primary forest in the world, based on estimates from the Forest Resource Assessment by the United Nations Food and Agriculture Organization [*FAO*, 2005]. Such extensive land use change has the potential to significantly alter catchment hydrology (in terms of both quantity and quality), with its effects sometimes not immediate but occurring gradually over a lengthy period of time. Recent estimates from satellite measurements indicate that rapid deforestation continues in the region, although at lower rates [e.g. *Kim et al.,* 2015]. Persistent land use change necessitates modelling methodologies that are capable of providing accurate hydrologic forecasts and predictions, despite non-stationarity in catchment processes. This is also particularly relevant for water resource management which requires reliable estimates of water availability, both in terms of volume and timing, to properly allocate the resource between different water uses and to prevent flood damages. Vietnam has built many reservoirs in the last decades and more are planned because they are considered to be fundamentally important for electricity production, flood control, water supply and irrigation, ultimately contributing to the development of the country [*Giuliani et al.*, 2016].

The literature on land-use change and its impacts on catchment hydrology is extensive, with studies examining the effects of 1) conversion to agricultural land-use [*Thanapakpawin et al*, 2007; *Warburton et al.,* 2012]; 2) deforestation [*Costa et al.,* 2003; *Coe et al*, 2011]; 3) afforestation [e.g. *Yang et al., 2012*; *Brown et al*, 2013] and urbanization [*Bhaduri et al.,* 2001; *Rose & Peters*, 2001].

Fewer studies have examined how traditional modelling approaches must be modified to handle non-stationary conditions, or how modelling methods can be used to assess impacts of land use change. Split sample calibration has been used frequently to retrospectively examine changes to model parameters due to land use or climatic change [*Seibert & McDonnell, 2010; Coron et al., 2012; McIntyre & Marshall*, 2010; *Legesse et al*, 2003]. Several other studies have employed scenario modelling, whereby hydrologic models are parameterized to represent different possible future land use conditions [e.g. *Niu & Sivakumar*, 2013; *Elfert & Borman*, 2010]. A related approach involves combining land use change forecast models with hydrologic models [e.g. *Wijesekara et al.,* 2012]. However the aforementioned approaches are unsuited to short-term predictive modelling or hydrologic forecasting in dynamic catchments, as the predicted land use change may not reflect actual changes. A potentially more suitable approach in such a setting is to allow model parameters to vary in time, rather than assuming a constant optimal value or stationary probability distribution. Many existing methods utilising such a framework require some *apriori* knowledge of the land use change in order to inform variations in model parameters (see for instance *Efstratiadis,* 2015; *Brown et al.,* 2006; and *Westra et al.,* 2014). Recent efforts have examined the potential for time varying models to automatically adapt to changing conditions using information contained in hydrologic observations and sequential Data Assimilation, without requiring explicit knowledge of the changes [see for example *Taver et al.,* 2015, *Pathiraja et al.,* 2016a&b]. Such approaches can objectively modify model parameters in response to signals of change in observations in real time, whilst simultaneously providing uncertainty estimates of parameters and streamflow predictions. T ~~T~~hey can also be used to determine whether ~~observed changes to streamflow dynamics are driven by climatic or land cover changes.~~ land cover changes (and not solely meteorological factors) contribute to observed changes in streamflow dynamics in retrospective studies where the lack of a paired control catchment precludes such an assessment.

Pathiraja et al. [2016a] presented an Ensemble Kalman Filter based algorithm (the so-called Locally

Linear Dual EnKF) to estimate time variations in model parameters. The method sequentially assimilates observations into a numerical model in real time to generate improved estimates of model states, fluxes and parameters at a given time based on their respective uncertainties. Its purpose is to infer changes to catchment properties (e.g. land cover change) from hydrologic observations, without prior knowledge of such changes, at the time scale of the observation frequency. It can therefore be used for various applications: 1) to retrospectively estimate time variations in model parameters; 2) for short-term predictive modelling (e.g. flood forecasting); and 3) for on-line/real time water resource management (e.g. determining releases from reservoirs in catchments with changing land cover conditions). When used for prediction, states and parameters are updated sequentially using all available observations up until the current time. These updated states and parameters are then used along with the prior parameter generating model to produce hydrologic predictions over a short time horizon. The efficacy of the method was demonstrated in *Pathiraja et al.* [2016b] through an ~~The method was~~ applied~~ed~~cation to small experimental catchments (< 350 ha) with drastic land cover changes and strong signals of change in streamflow observations.

Here we investigate two issues that are pertinent to modelling in realistic catchments with land use change. Firstly, we investigate the efficacy of the time varying parameter method for sparsely observed, larger catchments with gradual and spatially complex land use change. ~~Previous~~Several authors ~~studies~~ have demonstrated that impacts of land use change on the hydrologic response are dependent on many factors including the type and rate of land cover conversion as well the spatial pattern of different land uses within the catchment [*Dwarakish & Ganasri*, 2015; *Warburton et al.*, 2012]. In such situations, the effects of unresolved spatial heterogeneities in model inputs (e.g. rainfall) and the relatively less pronounced changes in land surface conditions make time varying parameter detection and accurate hydrologic prediction more difficult. The second objective is to ~~to 2 sets of small (< 350 ha) paired experimental catchments with rapid and extensive deforestation~~

~~(50% and 100% of catchment cleared over 3 months), leading to strong signals of change in the hydrologic observations [see *Pathiraja et al.*, 2016b]. Here we extend this work to a larger catchment experiencing more realistic land cover change (more gradual and patchy), whilst also investigating the importance of the chosen model structure. Previous studies have demonstrated that impacts of land use change on the hydrologic response are dependent on many factors including the type and rate of land cover conversion as well the spatial pattern of different land uses within the catchment [*Dwarakish & Ganasri*, 2015; *Warburton et al.*, 2012]. In such situations, the effects of unresolved spatial heterogeneities in model inputs (e.g. rainfall) and the relatively less pronounced changes in land surface conditions make time varying parameter detection more difficult. We also~~ ~~e~~examine the role of the hydrologic model in determining the ability of the time varying parameter framework to provide high quality predictions in changing conditions. Often there may be several candidate hydrologic models (with time invariant parameters) that have similar predictive performance for a catchment when calibrated and validated over a time series of static land cover conditions. This work examines whether all such candidate models in time varying parameter mode are also capable of providing accurate predictions under changing conditions.

~~–~~These issues are investigated for the Nammuc catchment (2880 km^2) in Northern Vietnam which has experienced deforestation largely due to increasing agricultural development. ~~Land cover change has occurred at varying rates, with cropland accounting for roughly 23% between 1981 and 1994, and 52% by 2000.~~ It serves as an ideal test catchment to study the efficacy of the time varying parameter algorithm due to its size, spatially complex pattern of land use changes, and lack of information on the precise timing of such changes. Land cover change is estimated to have ~~has~~ occurred at varying rates, with cropland accounting for roughly 23% between 1981 and 1994, and 52% by 2000. W~~w~~e also consider ~~use~~ two conceptual hydrologic models (given the availability of point rainfall, temperature, and streamflow data) to address the second objective. Both models ~~to~~demonstrate similar performance in representing streamflow at the outlet during the pre-change

period. The effect of the model structure on hydrologic predictions from the time varying parameter models is studied. ~~determine the ability of the Locally Linear Dual EnKF to produce accurate predictions under changing land surface conditions.~~

The remainder of this paper is structured as follows. Details of the study catchment and the impact of land cover change are analysed in Section 2. Section 3 summarizes the experimental setup including the hydrological models and the time varying parameter estimation method used. Results are provided in Section 4, along with an analysis of whether the time varying model structures reflect the observed catchment dynamics. Finally, we conclude with a summary of the main outcomes of the study as well as proposed future work.

2. The Nammuc Catchment

The Nammuc catchment (2880 km^2) is located in the Red River Basin, the second largest drainage basin in Vietnam which also drains parts of China and Laos. The local climate is tropical monsoon dominated with distinct wet (May to October) and dry (November to April) seasons. The wet season tends to have high temperatures (on average 27 to 29 °C) due to south-south easterly winds that bring humid air masses. Conversely, during the dry season, circulation patterns reverse carrying cooler dry air masses to the basin (leading to average temperatures of 16 to 21°C). Streamflow response is consequently monsoon driven, with high flows occurring between June and October (generally peaking in July/August) and low flows in the December to May period (Vu, 1993). Average annual rainfall at Nammuc varies between 1300 and 2000 mm (on average 1600 mm). A summary of catchment properties is provided in Table 1~~Table 1~~.

2.1.Data & Land Cover Change

Figure 1~~Figure 1~~ shows the available land cover information for the Nammuc catchment. The first land cover map refers to the period 1981-1994 and was obtained by the Vietnamese Forest Inventory and Planning Institute (http://fipi.vn/Home-en.htm). The second land cover map refers to year 2000 and was obtained from the FAO Global Land Cover database (http://www.fao.org/geonetwork/srv/en/metadata.show?id=12749&currTab=simple). A comparison of the two maps shows a reduction in forest cover in favor of cropland; Evergreen Leaf decreases from about 60% to 30% whilst cropland increases from about 23% to 52%. The change in land cover is patchy, although mostly concentrated in the northern part of the catchment. Because of the scant information available, it is not easy to identify the precise time period of these changes. Based on the available land cover map information and the changes to observed runoff (see Section 2.2~~2.1~~), we posit that a period of rapid extensive deforestation occurred in early-1990s.

Daily point rainfall data is available at four precipitation stations surrounding the catchment (Dien Bien, Tuan Giao, Quynh Nhai and Nammuc, see Figure 1~~Figure 1~~). Catchment averaged rainfall was developed as a weighted sum of the four stations with weights determined by Thiessen Polygons. Daily mean temperature was calculated in a similar fashion using temperature records from the 2 closest gauges (Lai Chau and Quynh Nhai, see Figure 1~~Figure 1~~). This was used to estimate Potential Evapotranspiration through the empirical temperature-latitude based Hamon PET method [*Hamon*, 1961]. Daily rainfall, temperature and streamflow data was provided by the Vietnamese Institute of Water Resources Planning.

~~2.1.~~2.2. Impact of Land Cover Change on Streamflow

An examination of the observed streamflow and rainfall records shows that distinct changes to the hydrologic regime are evident after the mid-1990s. The annual runoff coefficient varies between 0.4 and 0.6 prior to 1994, after which it increases to between 0.6 and 0.8 until 2004 (see Figure 2~~Figure 2~~a). However, increases to annual yields are driven mostly by changes to baseflow volume. This is

evident in Figure 2~~Figure 2~~a, which shows that the increase in the annual direct runoff coefficient $\left(\frac{runoff-baseflow}{rainfall}\right)$ is less than the increase in the total runoff coefficient (roughly 0.1 increase compared to 0.2 respectively). Baseflow was estimated using the two parameter recursive baseflow filter of *Eckhardt* [2005], with on-line updating of baseflow estimates to match low flows. A small increase in the Annual Baseflow Index $\left(\frac{baseflow}{runoff}\right)$ is apparent also, from about 0.32 on average in the period 1970 to 1982 to 0.39 on average after 1994 (Figure 2~~Figure 2~~b). This indicates that the annual increases to baseflow volume exceed the increases to direct runoff volume. Similar changes were found by *Wang et al.* [2012] who analyzed records in the entire Da River basin which drains the largest river in the Red River catchment.

At a seasonal time scale, it is apparent that both wet and dry season flows exhibit temporal variations. We utilized the Moving Average Shifting Horizon (MASH) [*Anghileri et al.,* 2014] and Mann-Kendall test to assess seasonal trends in observed streamflow, precipitation, and temperature data. The MASH tool can be used to qualitatively assess inter-annual variations in the seasonal pattern of a variable. It works by calculating a statistic of the data (e.g. mean) over the same block of days in consecutive years.~~–~~ A steady increase in baseflow is again apparent (see February to April in Figure 2~~Figure 2~~c), as well as increases to wet season flows (see June to September in Figure 2~~Figure 2~~c). Mann-Kendall test (with significance level equal to 5%) on annual and monthly streamflow time series shows increasing trends in almost all months, i.e., from October to July. No concurrent increases are apparent in rainfall (see Figure 2~~Figure 2~~d). Also the Mann-Kendall test applied to precipitation time series does not show any statistically significant trend, except a decrease in September for Nammuc and Quynh Nhai station and an increase in July for Dien Bien station. Temperature variations are not evident from the MASH analysis (not shown) and no significant trend can be detected by applying the Mann-Kendall test. These results indicate that changes in streamflow dynamics are likely due to land use change rather than climatic impacts.

3. Experimental Setup

3.1.Hydrologic Models

Conceptual lumped models were adopted due to the availability of point rather than distributed hydro-meteorological data of sufficient length. We considered the HyMOD [*Boyle*, 2001] and Hydrologiska Byrans Vattenbalansavdelning (HBV) [*Bergstrom et al.,* 1995] models. They differ mainly in the way components of the response flow are separated (HBV has near surface flow, interflow, and baseflow components whilst HyMOD has a quickflow and slow flow component only) and how these flows are routed. A schematic of the models is shown in Figure 3~~Figure 3~~.

In the HyMOD model, spatial variations in catchment soil storage capacity are represented by a Pareto distribution with shape parameter b and maximum point soil storage depth c_{max}. Excess rainfall (V) is partitioned into three cascading tanks representing quick flow and a single slow flow store through the splitting parameter α. Outflow from these linear routing tanks is controlled by parameters k_q (for the quick flow stores) and k_s (for the slow flow store). The model has a total of 5 states and 5 parameters.

In the HBV model, input to the soil store is represented by a power-law function (see Figure 3~~Figure 3~~, note the snow store is neglected for this study). Excess rainfall enters a shallow layer store which generates: 1) near surface flow (q_0) whenever the shallow store state ($stw1$) is above a threshold ($hl1$) and 2) interflow (q_1) by a linear routing mechanism controlled by the $K1$ parameter. Percolation from the shallow layer store to the deep layer store (controlled by $perc$ parameter) then leads to the generation of baseflow also via linear routing (controlled by the $K2$ parameter). Finally, a triangular weighting function of base length $Maxbas$ is used to route the sum of all three flow components. There are a total of 9 parameters and 3 states.

The Shuffled Complex Evolution Algorithm (SCE-UA) [*Duan et al.*, 1993] and the Borg Evolutionary Algorithm [*Hadka & Reed*, 2013] were used to calibrate the models to pre-change conditions (1973 to 1979). The period 1973 to 1979 was selected for calibration as it was expected to have minimal land cover changes, and also to ensure sufficient data availability for the assimilation period. Both models had very similar performance in terms of reproducing observed runoff (an NSE of 0.75 and 0.77 for HyMOD and HBV respectively). HBV was slightly better at reproducing low flows whilst HyMOD was slightly better at mid-range flows (see Table 2~~Table 2~~).

3.2. Time Varying Parameter Estimation

A Data Assimilation based framework for estimating time varying parameters was presented in *Pathiraja et al.* [2016a]. The approach relies on an Ensemble Kalman Filter (EnKF) [*Evensen*,1994] to perform sequential joint state and parameter updating. EnKFs were developed to extend the applicability of the celebrated Kalman Filter [*Kalman,* 1960] to non-linear systems, although they provide a sub-optimal update as only the mean and covariance are considered in generating the posterior. However they have been used with much success in many hydrologic applications [see for example *Reichle et al.,* 2002; *Gu et al.*, 2005; *Komma et al.,* 2008; *Sun et al.,* 2009; *Xu et al.,* 2016]. EnKFs offer a practical alternative to Sequential Monte Carlo/Particle Filter methods that propagate the full probability density through time, but suffer from several implementation issues even in moderate dimensional systems. ~~A framework for time varying parameter estimation based on Joint State and Parameter updating using the Ensemble Kalman Filter [*Evensen*, 1994] was presented in *Pathiraja et al.* [2016a].~~ The Locally Linear Dual EnKF method of *Pathiraja et al.* [2016a] works by sequentially proposing parameters, updating these using the Ensemble Kalman filter and available observations, and ~~then~~subsequently using these updated parameters to propose and update model states. An approach for proposing parameters in the time varying setting was also presented, for cases where no prior knowledge of parameter variations is available~~d, a task which is made difficult by the lack of a model that prescribes time variations in model parameters~~. The method ~~so-called~~

~~Locally Linear Dual EnKF~~ was verified against multiple synthetic case studies~~,~~ as well as ~~in~~for 2 small experimental catchments experiencing controlled land use change [*Pathiraja et al.,* 2016a and *Pathiraja et al.,* 2016b]. The algorithm is summarised below, for full details refer to *Pathiraja et al.* [2016a]~~ and 2016b]~~.

3.2.1. Locally Linear Dual EnKF

Suppose a dynamical system can be described by a vector of states $\boldsymbol{x}_t$ and outputs $\boldsymbol{y}_t$ and a vector of associated model parameters $\boldsymbol{\theta}_t$ at any given time *t.* The uncertain system states and parameters are represented by an ensemble of states $\{\boldsymbol{x}_t^i\}_{i=1:n}$ and parameters $\{\boldsymbol{\theta}_t^i\}_{i=1:n}$ each with *n* members. The prior state and parameter distributions $\{\boldsymbol{x}_t^{i-}\}_{i=1:n}$ and $\{\boldsymbol{\theta}_t^{i-}\}_{i=1:n}$ respectively represent our prior knowledge of the system, usually derived as the output from a numerical model.~~–~~ Suppose also that the system outputs are observed $(\boldsymbol{y}_t^o)$ but that there is also some uncertainty associated with these observations. The purpose of the data assimilation algorithm (here the EnKF) is to combine the prior estimates with measurements, based on their respective uncertainties, to obtain an improved estimate of the system states and parameters. ~~–~~A single cycle of the Locally Linear Dual EnKF procedure for a given time *t* is undertaken as follows~~:~~. Note in the following, the overbar notation is used to indicate the ensemble mean.

1. ***Propose ~~a set of~~a prior parameter ensembles~~.~~*** This involves generating a parameter ensemble using prior knowledge. In this case, our prior knowledge comes from the updated parameter ensemble from the previous time $(\boldsymbol{\theta}_{t-1}^{i+})$ and how it has changed over recent time steps. The assumed parameter dynamics is a Gaussian random walk with time varying mean and variance, given by:

$$\boldsymbol{\theta}_t^{i-} \sim N\left(\boldsymbol{\theta}_{t-1}^{i+} + \boldsymbol{m}_t, s^2\boldsymbol{\Sigma}_{t-1}^{\theta}\right) \; for\; i = 1{:}n \quad (1)$$

$$\boldsymbol{\Sigma}_{t-1}^{\theta} = \frac{1}{n-1}\sum_{i=1}^{n}\left(\boldsymbol{\theta}_{t-1}^{i+} - \overline{\boldsymbol{\theta}_{t-1}^{+}}\right)\left(\boldsymbol{\theta}_{t-1}^{i+} - \overline{\boldsymbol{\theta}_{t-1}^{+}}\right)^{\mathrm{T}} \quad (2)$$

where $\boldsymbol{\Sigma}_{t-1}^{\theta}$ is the sample covariance matrix of the updated parameter ensemble at time $t-1$; $\overline{\boldsymbol{\theta}_{t-1}^{+}}$ indicates the ensemble mean of the updated parameters at time $t-1$; ~~and~~ $(\,)^{\mathrm{T}}$ represents the transpose operator~~.~~; and s^2 is a tuning parameter. The prior ensemble mean is determined as the linear extrapolation of the updated ensemb~~ The prior (or background) ensemble ($\boldsymbol{\theta}_t^{i-}$) is generated by perturbing $\boldsymbol{\theta}_{t-1}^{i+}$ with random noise such that its mean is a linear extrapolation of updated ensemble me~~le mean~~ans from the previous two time steps, i.e.:

$$\boldsymbol{m}_t[k] = \begin{cases} \boldsymbol{m}_{t-1}[k], & |\boldsymbol{m}_{t-1}[k]| \le m_{max} \\ \boldsymbol{m}_{t-2}[k], & |\boldsymbol{m}_{t-1}[k]| > m_{max} \end{cases} \quad (3)$$

$$\boldsymbol{m}_{t-1} = \frac{\overline{\boldsymbol{\theta}_{t-1}^{+}} - \overline{\boldsymbol{\theta}_{t-2}^{+}}}{\Delta t} \quad (4)$$

$$\boldsymbol{m}_{t-2} = \frac{\overline{\boldsymbol{\theta}_{t-2}^{+}} - \overline{\boldsymbol{\theta}_{t-3}^{+}}}{\Delta t} \quad (5)$$

~~1.~~ ~~.~~ where $\boldsymbol{m}_t[k]$ indicates the kth component of the vector $\boldsymbol{m}_t$. ~~Perturbations are sampled from a Gaussian density with mean zero and variance $s^2\boldsymbol{\Sigma}_{t-1}^{\theta}$, where $\boldsymbol{\Sigma}_{t-1}^{\theta}$ is the covariance matrix of the updated parameter ensemble from the previous time and s^2 is a tuning parameter. The ensemble mean is then shifted to ensure it matches the linear extrapolation.~~ Note that the extrapolation is forced to be less than a pre-defined maximum rate of change m_{max} to minimise overfitting and avoid parameter drift due to isolated large updates.

2. ***Consider observation and forcing uncertainty.*** This is done by perturbing measurements of forcings and system outputs with random noise sampled from a distribution representing the ~~errors~~ uncertainty in those measurements. The result is an ensemble of forcings ($\boldsymbol{u}_t^i$) and observations ($\boldsymbol{y}_t^i$) each with *n* members. For example, if random errors in measurements of system outputs (herein also referred as observations) are characterized by a zero mean Gaussian distribution, the ensemble of observations is given by:

$$\boldsymbol{y}_t^i \sim N\left(\boldsymbol{y}_t^o, \boldsymbol{\Sigma}_t^{y^o y^o}\right) \; for\; i = 1{:}n \qquad (6)$$

~~2.~~ where $\boldsymbol{y}_t^o$ is the recorded measurement at time t and $\boldsymbol{\Sigma}_t^{y^o y^o}$ is the error covariance matrix of the measurements.

3. ***Generate simulations using prior parameters***. The prior parameters from Step 1, $\boldsymbol{\theta}_t^{i-}$ and updated states from the previous time, $\boldsymbol{x}_{t-1}^{i+}$ are forced through the model equations to generate an ensemble of model simulations of states ($\widehat{\boldsymbol{x}}_t^i$) ~~and~~ and outputs ($\widehat{\boldsymbol{y}}_t^i$~~).~~):

$$\widehat{\boldsymbol{x}}_t^i = f\left(\boldsymbol{x}_{t-1}^{i+}, \boldsymbol{\theta}_t^{i-}, \boldsymbol{u}_t^i\right) \; for\; i = 1{:}n \qquad (7)$$

$$\widehat{\boldsymbol{y}}_t^i = h\left(\widehat{\boldsymbol{x}}_t^i, \boldsymbol{\theta}_t^{i-}\right) \; for\; i = 1{:}n \qquad (8)$$

~~3.~~

4. ***Perform the Kalman update of parameters.*** Parameters are updated using the Kalman update equation and the prior parameter and simulated output ensemble from Step 1 and 3:

$$\boldsymbol{\theta}_t^{i+} = \boldsymbol{\theta}_t^{i-} + \mathbf{K}_t^{\theta}\left(\boldsymbol{y}_t^i - \widehat{\boldsymbol{y}}_t^i\right) \; for\; i = 1{:}n \qquad (9)$$

$$\mathbf{K}_t^{\theta} = \boldsymbol{\Sigma}_t^{\theta\hat{y}}\left[\boldsymbol{\Sigma}_t^{\hat{y}\hat{y}} + \boldsymbol{\Sigma}_t^{y^o y^o}\right]^{-1} \qquad (10)$$

~~4.~~

~~$\boldsymbol{\theta}_t^{i+} = \boldsymbol{\theta}_t^{i-} + \mathbf{K}_t^{\theta}\left(\boldsymbol{y}_t^i - \widehat{\boldsymbol{y}}_t^i\right) \; for\; i = 1{:}n \quad (1)$~~

~~$\mathbf{K}_t^{\theta} = \boldsymbol{\Sigma}_t^{\theta\hat{y}}\left[\boldsymbol{\Sigma}_t^{\hat{y}\hat{y}} + \boldsymbol{\Sigma}_t^{y^o y^o}\right]^{-1} \quad (2)$~~

where $\boldsymbol{\Sigma}_t^{\theta\hat{y}}$ is a matrix of the sample cross covariance between errors in parameters $\boldsymbol{\theta}_t^{i-}$ and simulated ~~observations~~ output $\widehat{\boldsymbol{y}}_t^i$; ~~$\boldsymbol{\Sigma}_t^{y^o y^o}$ is the error covariance matrix of the observations;~~ ~~a~~and $\boldsymbol{\Sigma}_t^{\hat{y}\hat{y}}$ is the sample error covariance matrix of the simulated ~~observations~~output:~~.~~

$$\boldsymbol{\Sigma}_t^{\theta\hat{y}} = \frac{1}{n-1}\sum_{i=1}^{n}\left(\boldsymbol{\theta}_t^{i-} - \overline{\boldsymbol{\theta}_t^{-}}\right)\left(\widehat{\boldsymbol{y}}_t^i - \overline{\widehat{\boldsymbol{y}}_t}\right)^{\mathrm{T}} \qquad (11)$$

$$\boldsymbol{\Sigma}_t^{\hat{y}\hat{y}} = \frac{1}{n-1}\sum_{i=1}^{n}\left(\widehat{\boldsymbol{y}}_t^i - \overline{\widehat{\boldsymbol{y}}_t}\right)\left(\widehat{\boldsymbol{y}}_t^i - \overline{\widehat{\boldsymbol{y}}_t}\right)^{\mathrm{T}} \qquad (12)$$

5. ***Generate simulations using updated parameters.*** Step 3 is repeated with the updated parameter ensemble $\boldsymbol{\theta}_t^{i+}$ to generate ~~an~~ the prior ensemble of model simulations of states ($\boldsymbol{x}_t^{i-}$) and outputs ($\tilde{\boldsymbol{y}}_t^i$):

$$\boldsymbol{x}_t^{i-} = f\left(\boldsymbol{x}_{t-1}^{i+}, \boldsymbol{\theta}_t^{i+}, \boldsymbol{u}_t^i\right) \; for\; i = 1{:}n \tag{13}$$

$$\tilde{\boldsymbol{y}}_t^i = h\left(\boldsymbol{x}_t^{i-}, \boldsymbol{\theta}_t^{i+}\right) \; for\; i = 1{:}n \tag{14}$$

~~5.~~

6. ***Perform the Kalman update of states and outputs***. Use the Kalman update equation for correlated measurement and process noise (equations 15 to 18) ~~,~~ and the simulated state ($\boldsymbol{x}_t^{i-}$) and output ($\tilde{\boldsymbol{y}}_t^i$) ensembles from Step 5 to update them~~:~~. Since the measurements have already been used to generate $\tilde{\boldsymbol{y}}_t^i$, the errors in model simulations and measurements are now correlated. The standard Kalman update equation (as in the form of equations 9 and 10) can no longer be used as it relies on the assumption that errors in measurements and model simulations are independent.

$$\boldsymbol{x}_t^{i+} = \boldsymbol{x}_t^{i-} + \mathbf{K}_t^x\left(\boldsymbol{y}_t^i - \tilde{\boldsymbol{y}}_t^i\right) \; for\; i = 1{:}n \tag{15}$$

$$\mathbf{K}_t^x = \left[\boldsymbol{\Sigma}_t^{x\tilde{y}} + \boldsymbol{\Sigma}_t^{\varepsilon_x y^o}\right]\left[\boldsymbol{\Sigma}_t^{\tilde{y}\tilde{y}} + \boldsymbol{\Sigma}_t^{\varepsilon_{\tilde{y}} y^o} + \left(\boldsymbol{\Sigma}_t^{\varepsilon_{\tilde{y}} y^o}\right)^{\mathrm{T}} + \boldsymbol{\Sigma}_t^{y^o y^o}\right]^{-1} \tag{16}$$

$$\boldsymbol{\varepsilon}_{x_t}^{\;i} = \boldsymbol{x}_t^{i-} - \hat{\boldsymbol{x}}_t^i \tag{17}$$

$$\boldsymbol{\varepsilon}_{\tilde{y}_t}^{\;i} = \tilde{\boldsymbol{y}}_t^i - \hat{\boldsymbol{y}}_t^i \tag{18}$$

~~6.~~

~~$$\boldsymbol{x}_t^{i+} = \boldsymbol{x}_t^{i-} + \mathbf{K}_t^x\left(\boldsymbol{y}_t^i - \tilde{\boldsymbol{y}}_t^i\right) \; for\; i = 1{:}n \quad (3)$$~~

~~$$\mathbf{K}_t^x = \left[\boldsymbol{\Sigma}_t^{x\tilde{y}} + \boldsymbol{\Sigma}_t^{\varepsilon_x y^o}\right]\left[\boldsymbol{\Sigma}_t^{\tilde{y}\tilde{y}} + \boldsymbol{\Sigma}_t^{\varepsilon_{\tilde{y}} y^o} + \left(\boldsymbol{\Sigma}_t^{\varepsilon_{\tilde{y}} y^o}\right)^{\mathrm{T}} + \boldsymbol{\Sigma}_t^{y^o y^o}\right]^{-1} \quad (4)$$~~

~~$$\boldsymbol{\varepsilon}_{x_t}^{\;i} = \boldsymbol{x}_t^{i-} - \hat{\boldsymbol{x}}_t^i \; ; \; \boldsymbol{\varepsilon}_{\tilde{y}_t}^{\;i} = \tilde{\boldsymbol{y}}_t^i - \hat{\boldsymbol{y}}_t^i \quad (5)$$~~

where $\boldsymbol{\Sigma}_t^{x\tilde{y}}$ is a matrix of the sample cross covariance between simulated states $\left\{\boldsymbol{x}_t^{i-}\right\}_{i=1:n}$ and outputs $\left\{\tilde{\boldsymbol{y}}_t^i\right\}_{i=1:n}$ from Step 5; $\boldsymbol{\Sigma}_t^{\varepsilon_x y^o}$ represents the sample covariance between

$\left\{\boldsymbol{\varepsilon}_{x_t}^{\,i}\right\}_{i=1:n}$ and the observations; and $\boldsymbol{\Sigma}_t^{\varepsilon_{\tilde{y}} y^o}$ represents the sample covariance between the $\left\{\boldsymbol{\varepsilon}_{\tilde{y}_t}^{\,i}\right\}_{i=1:n}$ and the observations~~;~~. ~~and $(\,)^{\mathrm{T}}$ represents the transpose operator.~~

The above algorithm specifies the updating of states and parameters at any given time, based on available observations. This allows one to retrospectively estimate time variations in model parameters, as well as provide one time step ahead forecasts of states & outputs (as per equations 7 and 8). Forecasts at longer time horizons would be made by generating prior parameters and states as detailed in Steps 1 to 3, although the local linear extrapolations are only valid close to the current time point.

~~3.2.1.~~3.2.2. Application to the Nammuc Catchment

Joint state and parameter estimation was undertaken for the Nammuc Catchment over the period 1975 to 2004 by assimilating streamflow observations into the HyMOD and HBV models at a daily time step. Given the fairly low parameter dimensionality of HyMOD, all model parameters were allowed to vary in time whilst for HBV the lp and $Maxbas$ parameters (see Figure 3~~Figure 3~~) were held fixed (lp = 1 and $Maxbas$ = 1 day). This was based on the results of Variance Based Sensitivity Analysis or Sobol method [see for example *Saltelli et al.,* 2008] implemented through the SAFE toolbox [*Pianosi et al.,* 2015] which found these to be the least sensitive and least important in defining variations to catchment hydrology (see Table 3~~Table 3~~). Note that although the $hl1$ parameter was found to have low sensitivity, it was retained as a time varying parameter due to its conceptual importance in separating interflow and near surface flow (refer Figure 3~~Figure 3~~).

Unbiased normally distributed ensembles of the parameters and states are required to initialise the LL Dual EnKF. Initial parameter ensembles were generated by sampling from a Gaussian distribution with mean equal to the calibrated parameters over the pre-change period and variance estimated from parameter sets with similar objective function values. Parameter sets with similar objective

function values were obtained when using different starting points to the optimization algorithm during the model calibration stage. Initial state ensembles were also sampled from normal distributions with mean equal to the simulated state at the end of the calibration period. An ensemble size of 100 members was adopted and assumed sufficiently large based on the findings of *Moradkhani et al.* [2005] and *Aksoy et al.* [2006]. Due to the stochastic-dynamic nature of the method, ensemble statistics were calculated over 20 separate realisations of the LL Dual EnKF. The prior parameter generating method described in Step 1 of Section 3.2~~3.2~~ requires specification of the tuning parameter s^2 to define the variance of the perturbations. This was tuned by selecting the s^2 value that optimized the quality of forecast streamflow over the calibration period. Forecast quality was assessed using the ~~optimized the~~ logarithmic score (LS) [*Good,* 1952] ~~(a measure of forecast quality)~~ of background streamflow predictions ($\tilde{y}_t^i$) using updated parameters (equation 14) ~~obtained from the LL Dual EnKF~~, which was averaged over the calibration period of length *T*:

$$\overline{LS} = \sum_{t=1}^{T} LS_t \quad (19)$$

$$LS_t = \log\left(f(y = y_t^o)\right) \quad (20)$$

~~log~~ where $f(y)$ is the probability density function of the background streamflow predictions (represented by the empirical pdf of the sample points $\{\tilde{y}_t^i\}_{i=1:n}$); and y_t^o is the measurement of the system outputs. The s^2 value that gave the largest $\overline{LS}$ was adopted for the assimilation period. ~~.~~ The maximum allowable daily rate of change in the ensemble mean was based on assuming a linear rate of change within the entire feasible parameter space over a three year period.

As detailed in Section 3.2~~3.2~~, observation and forcing uncertainty is considered by perturbing measurements with random noise. Here streamflow errors were assumed to be zero-mean normally distributed (truncated to ensure positivity) and heteroscedastic. The variance is defined as a proportion of the observed streamflow, to reflect the fact that larger flows tend to have greater errors than low flows:

$$y_t^i \sim TN(y_t^o, d.y_t^o) \ \ for\ i = 1:n \quad (21)$$

~~$$q_{obs}^i(t) = q_{obs}(t) + \varepsilon_q^i \ where\ \varepsilon_q^i \sim TN\left(0, d \times q_{obs}(t)\right) \quad i = 1:n \quad (6)$$~~

where TN indicates the truncated normal distribution to ensure positive flows and d = 0.1. A multiplier of 0.1 was chosen based on estimates adopted for similar gauges in hydrologic DA studies [e.g. *Clark et al.,* 2008; *Weerts & Serafy,* 2006; *Xie et al.,* 2014].

Several studies have noted that a major source of rainfall uncertainty arises from scaling point rainfall to the catchment scale [*Villarini & Krajewski*, 2008; *McMillan et al.*, 2011] and that multiplicative errors models are suited to describing such errors [e.g. *Kavetski et al.*, 2006]. Rainfall uncertainties were therefore described using unbiased, lognormally distributed multipliers:

$$P_t^i = P_t.M^i \quad (22)$$

$$M^i \sim LN(m, v) \text{ and } X^i = \log\left(M^i\right) \sim N(\mu, \sigma^2) \quad for\ i = 1:n \quad (23)$$

~~$$P^i(t) = P(t).M^i \quad (7)$$~~

~~$$M^i \sim LN(m, v) \text{ and } X^i = \log\left(M^i\right) \sim N(\mu, \sigma^2) \quad i = 1:n \quad (8)$$~~

where P_t is the measured rainfall at time t; ~~,~~ m and v are the mean and variance of the lognormally distributed rainfall multipliers M respectively; and μ and σ^2 are the mean and variance of the normally distributed logarithm of the rainfall multipliers M. For unbiased perturbations, we let m = 1. The variance of the rainfall multipliers (v) was estimated by considering upper and lower bound error estimates in the Thiessen weights assigned to the four rainfall stations (see Section 2.1~~2~~ for calculation of catchment averaged rainfall, ~~$P(t)$~~P_t). The resulting upper and lower bound catchment averaged rainfall ~~sequences~~ data were then used to estimate error parameters due to spatial variation in rainfall:

$$v = e^{(2\mu + \sigma^2)}.\left(e^{\sigma^2} - 1\right) \quad (24)$$

$$\sigma^2 = \widehat{\sigma^2} = var\left(\log\left[\frac{P_{upper,10}}{P_{lower,10}}\right]\right) \quad (25)$$

$$\mu = \log(m) - \frac{\sigma^2}{2} = -\frac{\sigma^2}{2} \quad (26)$$

~~$v = e^{(2\mu+\sigma^2)}.(e^{\sigma^2} - 1)$ (9)~~

~~$\sigma^2 = \widehat{\sigma^2} = var\left(\log\left[\frac{P_{upper,10}}{P_{lower,10}}\right]\right)$ (10)~~

~~$\mu = \log(m) - \frac{\sigma^2}{2} = -\frac{\sigma^2}{2}$ (11)~~

where $P_{upper,10}$ indicates catchment averaged rainfall data ~~sequence~~ estimated using the upper bound Thiessen weights with daily depth greater than 10mm (similar for $P_{lower,10}$) ~~an. d~~ $\widehat{\sigma^2}$ ~~was found to be 0.05.~~ A 10mm rainfall depth threshold was chosen to avoid large rainfall fractions due to small rainfall depths. $\widehat{\sigma^2}$ was found to be 0.05 in this case study. Similarly, we assume the dominant source of uncertainty in temperature data arises from spatial variation. Differences in temperature records at Lai Chau and Quynh Nhai (only available gauges with temperature records) were analysed and found to be approximately normally distributed with sample mean 0.2 deg C and variance of 1.4 deg C. A perturbed temperature ensemble was then generated according to equation 27~~13~~:

$$T_t^i \sim TN\left(T_t^{avg}, 1.4\right) \quad for \;\; i = 1{:}n \quad (27)$$

~~$T^i(t) = T_{avg}(t) + \varepsilon_T^i \; where \; \varepsilon_T^i \sim TN(0, 1.4) \quad i = 1{:}n$ (12)~~

where T_t^{avg} ~~$T_{avg}(t)$~~ represents catchment averaged temperature data (see Section 2.1~~2~~). Note that perturbations were taken to be unbiased (zero mean) as the sample mean of the differences in the temperature records was close to zero. The same perturbed input and observation sequences were

used for the HyMOD and HBV runs for the sake of comparison. A summary of the values adopted for the various components of the Locally Linear Dual EnKF for each model is provided in Table 4~~Table 4~~ and Table 5~~Table 5~~.

4. Results and Discussion

Temporal ~~V~~variations in the estimated parameter distributions from the LL Dual EnKF are evident for both models. In the case of the HBV model, changes at an inter-annual time scale are evident for the $perc$ and β (see Figure 4~~Figure 4~~). The decrease in the β parameter means that a greater proportion of rainfall is converted to runoff (i.e. more water entering the shallow layer storage). Additionally, the increase in the $perc$ parameter means that a greater volume of water is made available for baseflow generation. These changes correspond with the observed increase in the annual runoff coefficient (Figure 2~~Figure 2~~) and increase in baseflow volume (as discussed in Section 2.2~~2.1~~). Similar parameter adjustments are seen for HyMOD, at least at a qualitative level (see Figure 5~~Figure 5~~). The sharp increase in the b parameter during the post-change period means that a greater volume of water is available for routing (as larger b values mean that a smaller proportion of the catchment has deep soil storage capacity) and the downward inter-annual trend in α means that a greater portion of excess runoff is routed through the baseflow store. Intra-annual variations in updated model parameters for both HyMOD and HBV are also apparent (refer Figure 4~~Figure 4~~ and Figure 5~~Figure 5~~). This is due to the inability of a single parameter distribution to accurately model both wet and dry season flows, an issue that is commonly encountered when modelling large heterogeneous catchments experiencing significant spatial variation in rainfall. Such variations were not observed when using the time varying parameter framework for small deforested catchments (< 350ha) [see *Pathiraja et al.,* 2016b]. The comparatively less clear parameter changes for the Nammuc catchment are due to a combination of the increased difficulty in accurately modelling the hydrologic response (even in pre-change conditions) and due to the relatively more subtle and

gradual changes to land cover. Nonetheless, the method is shown to generate a temporally varying structure that is conceptually representative of the observed changes.

Despite the overall correspondence between changes to model parameters and observed streamflow, a closer examination shows that the hydrologic model structure is critical in determining whether the time varying parameter models accurately reflect changes in all aspects of the hydrologic response (not just total streamflow). In order to examine the impact of parameter variations on the model dynamics, we generated model simulations with the time varying parameter ensemble from the LL Dual EnKF, but without state updating (hereafter referred to as TVP-HBV and TVP-HyMOD). Streamflow predictions from the LL Dual EnKF (i.e. with state and parameter updating) for both the HyMOD and HBV are generally of similar quality and superior to those from the respective time invariant parameter models, although a slight bias in baseflow predictions from HyMOD is evident (see for example Figure 6~~Figure 6~~). However, differences in predictions from TVP-HBV and TVP-HyMOD are more striking due to the lack of state updating. Figure 7~~Figure 7~~ shows annual statistics of simulated streamflow from the TVP-HBV and TVP-HyMOD models and observed runoff. The TVP-HBV gives direct runoff and baseflow predictions that are consistent with runoff observations, meaning that the parameter adjustments reflect the observed changes in the runoff response. This however is not the case for the TVP-HyMOD. The annual runoff coefficient and annual direct runoff coefficient are severely under-estimated in the post-change period by the TVP-HyMOD, whilst the Annual Baseflow Index has an increasing trend of magnitude far greater than observed (Figure 7~~Figure 7~~c). All three quantities on the other hand are well represented by the TVP-HBV (Figure 7~~Figure 7~~).

Similar conclusions can be drawn from Figure 8~~Figure 8~~, which shows the results of a Moving Average Shifting Horizon (MASH) analysis (see Section 2.2~~2.1~~) on total and direct runoff (observed and simulated). Observed increases in January to April flows (see Figure 8~~Figure 8~~a) and wet season

direct flows (July to September) (see Figure 8~~Figure 8~~e) are well represented by the TVP-HBV but not TVP-HyMOD. The reason for these differences between the two models lies in their structure. In joint state-parameter updating using HyMOD, underestimated runoff predictions during recession periods lead to adjustments to the k_s and α parameters to increase baseflow depth. Unlike HBV, HyMOD has no continuous supply of water to the routing stores (i.e. the quick flow and slow flow stores) during recession periods (which typically have extended periods of no rainfall, so that V in Figure 3~~Figure 3~~ is zero). This means that k_s and α are updated to extreme values to compensate for the volumetric shortfall. HBV on the other hand has a continuous percolation of water into the deep layer store even during periods of no rain (so long as the shallow water store is non-empty). In summary, the HyMOD model structure prevents the parameters from being updated to values that realistically reflect the observed changes to catchment dynamics.

Having established that the TVP-HBV provided a good representation of the observed streamflow dynamics, we used a modelling approach to determine whether the observed changes were solely driven by forcings ~~climatically driven~~ and which (if any) components of runoff were also affected by land use change. A resampled rainfall and temperature time series was generated by sampling the data without replacement across years for each day (for instance rainfall and temperature for 1st January 1990 is found by randomly sampling from all records on 1st January). This maintains the intra-annual (e.g. seasonal) variability but destroys any inter-annual trends in the meteorological data. Streamflow simulations were then generated using this resampled meteorological sequence as inputs to the TVP-HBV (i.e. without state updating). If the resulting streamflow simulations do not reproduce the observed changes to streamflow dynamics, then this indicates that changes to meteorological forcings are the main contributor. However, if it is able to at least partially (or fully) reproduce the observed streamflow changes, this means that land cover changes are impacting catchment hydrology (but potentially in addition to forcing changes, due to the presence of ecosystem feedbacks). –Figure 8~~Figure 8~~d&h show the results of a MASH undertaken on the

resulting simulations of total and direct runoff using the resampled forcing time series and TVP-HBV model. Observed increases in baseflow during the January – April period (see Figure 8~~Figure 8~~a) and increases in direct runoff in the June – September period (see Figure 8~~Figure 8~~e) are reproduced. The magnitude of increase in direct runoff in July is slightly lower, indicating the potential for some climatic influences also. This is consistent with findings from the Mann-Kendall test which identified a statistically significant increase in July rainfall (see Section 2.2~~2.1~~). Overall however, these results lend further weight to the conclusion that land cover change has impacted the hydrologic regime of the Nammuc catchment. These results also demonstrate that parameter changes correspond to actual changes in catchment hydrology, and are not just random fluctuations that reproduce the observed streamflow statistics only when the observed forcing time series is used.

5. Conclusions

As our anthropogenic footprint expands, it will become increasingly important to develop modelling methodologies that are capable of handling dynamic catchment conditions. Previous work proposed the use of models whose parameters vary with time in response to signals of change in observations. The so-called Locally Linear Dual EnKF time varying parameter estimation algorithm [*Pathiraja et al.,* 2016a] was applied to 2 sets of small (< 350 ha) paired experimental catchments with deforestation occurring under experimental conditions (rapid clearing of 100% and 50% of land surface) [*Pathiraja et al.,* 2016b]. Here we demonstrate the efficacy of the method for a larger catchment experiencing more realistic land cover change, whilst also investigating the importance of the chosen model structure in ensuring the success of time varying parameter methods. We also demonstrate that the time varying parameter framework can be used in a retrospective fashion to determine whether ~~changes to the hydrologic regime are a result of climatic or land cover changes.~~ land cover changes (and not just meteorological factors) contribute to the observed hydrologic changes.

Experiments were undertaken on the Nammuc catchment (2880 km^2) in Vietnam, which experienced a relatively gradual conversion from forest to cropland over a number of years (cropland increased from roughly 23% of the catchment between 1981 and 1994 to 52% by 2000). Changes to the hydrologic regime after the mid-1990s were detected and attributed mostly to an increase in baseflow volume. Application of the LL Dual EnKF with two conceptual models (HBV and HyMOD) showed that the time varying parameter framework with state updating improved streamflow prediction in post-change conditions compared to the time invariant parameter case. However, baseflow predictions from the LL Dual EnKF with HBV were generally superior to the HyMOD case which tended to have a slight negative bias. It was found that the structure (i.e. model equations) of HyMOD was unsuited to representing the modified baseflow conditions, resulting in extreme and unrealistic time varying parameter estimates. This work shows that the chosen model is critical for ensuring the time varying parameter framework successfully models streamflow in unknown future land cover conditions. Appropriate model selection can be a difficult task due to the significant uncertainty associated with future land use change, and can be even more problematic when multiple models have similar performance in pre-change conditions (as was the case in this study). One possible way to ensure success of the time varying parameter approach is to use physically based models whose fundamental equations more closely model physical processes (for instance, modelling sub-surface flow using Richard's equation with hydraulic conductivity allowed to vary with time). The drawback of such approaches is that they are generally data intensive, both in generating model simulations (i.e. detailed inputs) and specifying parameters. Another possibility is to combine time varying parameter framework with multi-model approaches.

6. Acknowledgements

This study was funded by the Australian Research Council as part of the Discovery Project DP140102394. Dr Marshall is additionally supported through a Future Fellowship FT120100269.

534 The data used in this paper were collected under the project IMRR (Integrated and sustainable water
535 Management of Red Thai Binh Rivers System in changing climate), funded by the Italian Ministry of
536 Foreign Affairs (Delibera n. 142 del 8 Novembre 2010). We greatly acknowledge Dr. Andrea
537 Castelletti for provision of data and for discussions on this work.

538

539 Data utilized in this study can be made available from the authors upon request.

7. References

Aksoy, A., Zhang, F., Nielsen-Gammon, J. (2006). Ensemble-Based Simultaneous State and Parameter Estimation in a Two-Dimensional Sea-Breeze Model. *Monthly Weather Review*, 134, 2951–2970.

Anghileri, D., Pianosi, F., & Soncini-Sessa, R. (2014). Trend detection in seasonal data: From hydrology to water resources. *Journal of Hydrology*, *511*, 171–179. http://doi.org/10.1016/j.jhydrol.2014.01.022

Bergström, S. 1995. The HBV model. In: Singh, V.P. (Ed.) *Computer Models of Watershed Hydrology*. Water Resources Publications, Highlands Ranch, CO., pp. 443-476.

Bhaduri, B. B., Minner, M., Tatalovich, S., Member, A., & Harbor, J. (2001). Long-term hydrologic impact of urbanization: A tale of two models. *Journal of Water Resources Planning and Management*, *127*(February), 13–19.

Boyle, D. (2001). Multicriteria calibration of hydrological models, *Ph.D. dissertation*, Univ. of Ariz., Tucson.

Brown, A. E., Mcmahon, T. A., Podger, G. M., & Zhang, L. (2006). A methodology to predict the impact of changes in forest cover on flow duration curves, *CSIRO Land and Water Science Report 8/06*.

Brown, A. E., Western, A. W., McMahon, T. a., & Zhang, L. (2013). Impact of forest cover changes on annual streamflow and flow duration curves. *Journal of Hydrology*, *483*, 39–50. http://doi.org/10.1016/j.jhydrol.2012.12.031

Clark, M. P., Rupp, D. E., Woods, R. A., Zheng, X., Ibbitt, R. P., Slater, A. G., … Uddstrom, M. J. (2008). Hydrological data assimilation with the ensemble Kalman filter: Use of streamflow observations to update states in a distributed hydrological model. *Advances in Water Resources*, *31*(10), 1309–1324. http://doi.org/10.1016/j.advwatres.2008.06.005

Coe, M. T., Latrubesse, E. M., Ferreira, M. E., & Amsler, M. L. (2011). The effects of deforestation and climate variability on the streamflow of the Araguaia River, Brazil. *Biogeochemistry*, *105*(1–3), 119–131. http://doi.org/10.1007/s10533-011-9582-2

Coron, L., Andréassian, V., Perrin, C., Lerat, J., Vaze, J., Bourqui, M., & Hendrickx, F. (2012). Crash testing hydrological models in contrasted climate conditions: An experiment on 216 Australian catchments. *Water Resources Research,* 48(5), 1–17. doi:10.1029/2011WR011721

Costa, M. H., Botta, A., & Cardille, J. A. (2003). Effects of large-scale changes in land cover on the discharge of the Tocantins River, Southeastern Amazonia. *Journal of Hydrology*, *283*(1–4), 206–217. http://doi.org/10.1016/S0022-1694(03)00267-1

Duan, Q. Y., Gupta, V. K., & Sorooshian, S. (1993). Shuffled complex evolution approach for effective and efficient global minimization. *Journal of Optimization Theory and Applications*, *76*(3), 501–521. doi:10.1007/BF00939380

Dwarakish, G. S., & Ganasri, B. P. (2015). Impact of land use change on hydrological systems: A review of current modeling approaches. *Cogent Geoscience*, *1*(1), 1115691–1115691. http://doi.org/10.1080/23312041.2015.1115691

577 Eckhardt, K. (2005). How to construct recursive digital filters for baseflow separation. *Hydrological*
578 *Processes*, *19*(2), 507–515. http://doi.org/10.1002/hyp.5675

579 Efstratiadis, A., Nalbantis, I., & Koutsoyiannis, D. (2015). Hydrological modelling of temporally-varying
580 catchments: facets of change and the value of information. *Hydrological Sciences Journal*, *60*(7–
581 8), 1438–1461. http://doi.org/10.1080/02626667.2014.982123

582 Elfert, S., & Bormann, H. (2010). Simulated impact of past and possible future land use changes on
583 the hydrological response of the Northern German lowland "Hunte" catchment. *Journal of*
584 *Hydrology*, 383, 245–255. http://dx.doi.org/10.1016/j.jhydrol.2009.12.040

585 Evensen, G. (1994). Sequential data assimilation with a nonlinear quasi-geostrophic model using
586 Monte Carlo methods to forecast error statistics. *Journal of Geophysical Research*, *99*(C5).
587 http://doi.org/10.1029/94JC00572

588 FAO (2005). Global Forest Resources Assessment 2005 (FRA 2005)

589 Good, I.J. (1952). Rational Decisions. *Journal of the Royal Statistical Society.* B 14: 107–114.
590
591 Gu, Y., and D. S. Oliver (2005), History matching of the PUNQ-S3 reservoir model using the ensemble
592 Kalman filter, *SPE J.*, *10*(2), 217–224, doi:10.2118/89942-PA.
593
594 Giuliani, M., Anghileri, D., Castelletti, A., Vu, P. N., & Soncini-Sessa, R. (2016). Large storage
595 operations under climate change: expanding uncertainties and evolving tradeoffs.
596 *Environmental Research Letters*, 11(3), 035009.
597
598
599 Hadka, D., Reed, P., (2013). Borg: an auto–adaptive many–objective evolutionary computing
600 framework. *Evol. Comput*. 21 (2), 231–259.

601 Hamon, W. (1961). Estimating potential evapotranspiration. *Transactions of the American Society of*
602 *Civil Engineers*, 128(1), pp.324-337.

603 Kalman, R.E. (1960) A new approach to linear filtering and prediction problems, Transactions of the
604 ASME – *Journal of Basic Engineering*, Series D, 82 (1960), 35–45.

605 Kavetski, D., Kuczera, G., & Franks, S. W. (2006). Bayesian analysis of input uncertainty in hydrological
606 modeling: 1. Theory. *Water Resources Research*, *42*(3), n/a–n/a. doi:10.1029/2005WR004368
607
608 Kim, D.-H., J. O. Sexton, and J. R. Townshend (2015). Accelerated deforestation in the humid tropics
609 from the 1990s to the 2000s, *Geophysical Research Letters*, 42, 3495–3501, doi:10.1002/
610 2014GL062777.

611 Komma, J., G. Blöschl, and C. Reszler (2008), Soil moisture updating by Ensemble Kalman Filtering in
612 real-time flood forecasting, *J. Hydrol.*, *357*(3–4), 228–242, doi:10.1016/j.jhydrol.2008.05.020.
613
614

615
616 Kummer, D., and Turner, B. (1994). The Human Causes of Deforestation in Southeast Asia. *BioScience,*
617 *44*(5), 323-328. doi:10.2307/1312382

618
619 Legesse, D., Vallet-Coulomb, C., & Gasse, F. (2003). Hydrological response of a catchment to climate
620 and land-use changes in Tropical Africa: case study South Central Ethiopia. *Journal of Hydrology*,
621 *275*(1-2), 67–85. doi:10.1016/S0022-1694(03)00019-2
622
623 McIntyre, N., & Marshall, M. (2010). Identification of rural land management signals in runoff
624 response. *Hydrological Processes*, *24*(24), 3521–3534. doi:10.1002/hyp.7774
625
626 McMillan, H., Jackson, B., Clark, M., Kavetski, D., & Woods, R. (2011). Rainfall uncertainty in
627 hydrological modelling: An evaluation of multiplicative error models. *Journal of Hydrology*,
628 *400*(1-2), 83–94. doi:10.1016/j.jhydrol.2011.01.026

629 Moradkhani, H., Sorooshian, S., Gupta, H. V., & Houser, P. R. (2005). Dual state–parameter
630 estimation of hydrological models using ensemble Kalman filter. *Advances in Water Resources*,
631 *28*(2), 135–147. http://doi.org/10.1016/j.advwatres.2004.09.002

632 Niu, J., & Sivakumar, B. (2013). Study of runoff response to land use change in the East River basin in
633 South China. *Stochastic Environmental Research and Risk Assessment*. doi:10.1007/s00477-013-
634 0690-5

635 Pathiraja, S., Marshall, L., Sharma, A., & Moradkhani, H. (2016a). Hydrologic modeling in dynamic
636 catchments: A data assimilation approach. *Water Resources Research*, *52*, 3350–3372.
637 http://doi.org/10.1002/2015WR017192

638 Pathiraja, S., Marshall, L., Sharma, a., & Moradkhani, H. (2016b). Detecting non-stationary hydrologic
639 model parameters in a paired catchment system using data assimilation. *Advances in Water*
640 *Resources*, *94*, 103–119. http://doi.org/10.1016/j.advwatres.2016.04.021

641 Pianosi, F., Sarrazin, F., Wagener, T. A Matlab toolbox for Global Sensitivity Analysis, *Environmental*
642 *Modelling & Software*, 70, 80-85, http://dx.doi.org/10.1016/j.envsoft.2015.04.009.

643 Reichle, R. H., D. B. McLaughlin, and D. Entekhabi (2002), Hydrologic Data Assimilation with the
644 Ensemble Kalman Filter, *Am. Meteorol. Soc. - Mon. Weather Rev.*, *130*(1), 103–114,
645 doi:10.1175/1520-0493(2002)130<0103:HDAWTE>2.0.CO;2.
646

647 Rose, S., & Peters, N. E. (2001). Effects of urbanization on streamflow in the Atlanta area (Georgia,
648 USA): a comparative hydrological approach. *Hydrological Processes*, *15*(8), 1441–1457.
649 http://doi.org/10.1002/hyp.218

650

651 Saltelli, A., Ratto, M., Andres, T., Campolongo, F., Cariboni, J., Gatelli, D., Saisana, M., Tarantola, S.,
652 (2008). Global Sensitivity Analysis, the Primer. Wiley.

653 Seibert, J., & McDonnell, J. J. (2010). Land-cover impacts on streamflow: a change-detection
654 modelling approach that incorporates parameter uncertainty. *Hydrological Sciences Journal*,
655 *55*(3), 316–332. doi:10.1080/02626661003683264
656

Sun, A. Y., A. Morris, and S. Mohanty (2009), Comparison of deterministic ensemble Kalman filters for assimilating hydrogeological data, *Adv. Water Resour.*, *32*(2), 280–292, doi:10.1016/j.advwatres.2008.11.006.

Taver, V., Johannet, a., Borrell-Estupina, V., & Pistre, S. (2015). Feed-forward vs recurrent neural network models for non-stationarity modelling using data assimilation and adaptivity. *Hydrological Sciences Journal*, *60*(7–8), 1242–1265. http://doi.org/10.1080/02626667.2014.967696

Thanapakpawin, P., Richey, J., Thomas, D., Rodda, S., Campbell, B., & Logsdon, M. (2007). Effects of landuse change on the hydrologic regime of the Mae Chaem river basin, NW Thailand. *Journal of Hydrology*, *334*(1-2), 215–230. doi:10.1016/j.jhydrol.2006.10.012

Villarini, G., & Krajewski, W. F. (2008). Empirically-based modeling of spatial sampling uncertainties associated with rainfall measurements by rain gauges. *Advances in Water Resources*, *31*(7), 1015–1023. doi:10.1016/j.advwatres.2008.04.007

Vu, V.T., 1993. Evaluation of the impact of deforestation to inflow regime of the Hoa Binh Reservoir in Vietnam, Hydrology of Warm Humid Regions (Proceedings of the Yokohama Symposium, July 1993). IAHS Publ. no. 216

Wang, J., Ishidaira, H., & Xu, Z. X. (2012). Effects of climate change and human activities on inflow into the Hoabinh Reservoir in the Red River basin. *Procedia Environmental Sciences*, *13*, 1688-1698.

Warburton, M. L., Schulze, R. E., & Jewitt, G. P. W. (2012). Hydrological impacts of land use change in three diverse South African catchments. *Journal of Hydrology*, *414–415*, 118–135. http://doi.org/10.1016/j.jhydrol.2011.10.028

Weerts, A. H., & El Serafy, G. Y. H. (2006). Particle filtering and ensemble Kalman filtering for state updating with hydrological conceptual rainfall-runoff models. *Water Resources Research*, *42*(9), n/a-n/a. http://doi.org/10.1029/2005WR004093

Westra, S.; Thyer, M.; Leonard, M.; Kavetski, D.; Lambert, M. (2014). A strategy for diagnosing and interpreting hydrological model nonstationarity. *Water Resources Research*, 5090–5113. http://doi.org/10.1002/2013WR014719.Received

Wijesekara, G. N., Gupta, A., Valeo, C., Hasbani, J. G., Qiao, Y., Delaney, P., & Marceau, D. J. (2012). Assessing the impact of future land-use changes on hydrological processes in the Elbow River watershed in southern Alberta, Canada. *Journal of Hydrology*, *412–413*, 220–232. http://doi.org/10.1016/j.jhydrol.2011.04.018

WWF. (2013). Ecosystems in the Greater Mekong: Past trends, current status, possible futures.

Xie, X., Meng, S., Liang, S., & Yao, Y. (2014). Improving streamflow predictions at ungauged locations with real-time updating: application of an EnKF-based state-parameter estimation strategy. *Hydrology and Earth System Sciences*, *18*(10), 3923–3936. http://doi.org/10.5194/hess-18-3923-2014

698 Xu, T., and J. . Gomez-Hernandez (2016), Joint identification of contaminant source location, initial
699 release time, and initial solute concentration in an aquifer via ensemble kalman filtering, *Water*
700 *Resour. Res.*, 600–612, doi:10.1002/2015WR018249.

701

702 Yang, L., Wei, W., Chen, L., & Mo, B. (2012). Response of deep soil moisture to land use and
703 afforestation in the semi-arid Loess Plateau, China. *Journal of Hydrology*, *475*, 111–122.
704 http://doi.org/10.1016/j.jhydrol.2012.09.041

Tables

	Pre 1994	Post 1994
Land Use		
Evergreen Forest (including evergreen needle and evergreen leaf) (%)	77%	48%
Cropland (%)	23%	52%
Hydro-Meteorological Properties		
Mean Annual Rainfall (mm)	1630	1660
Mean Annual Runoff (mm)	838	1190
Mean Annual Runoff Coefficient	0.5	0.7
Mean Annual PET (mm)	1300	1300

Table 1 Study catchment properties

	HYMOD	HBV
NSE [ ]	**0.77**	0.75
Peak flows (q > 5mm/d)		
MAE [mm/d]	3.11	**2.85**
RMSE [mm/d]	**4.55**	4.72
Medium flows (1 mm/d <= q <= 5mm/d)		
MAE [mm/d]	**0.66**	0.80
RMSE [mm/d]	**0.86**	1.09
Low flows (q < 1mm/d)		
MAE [mm/d]	0.35	**0.20**
RMSE [mm/d]	0.42	**0.34**

Table 2 Model performance in pre-change conditions (1975 – 1979). Bold face numbers correspond to the model with superior performance for the particular metric.

	Sensitivity Index
hl1	0.10
lp	0.12
Maxbas	0.14
fcap	0.18
K0	0.23
K2	0.23
K1	0.38
beta	0.41
perc	0.47

Table 3 Variance Based Sensitivity Analysis Results for HBV parameters: first order sensitivity index representing the contribution of varying a single parameter to the variance of the model output. Lower values indicate lower sensitivity.

727

	Description	Units	Initial Sampling Distribution	Feasible Range	~~Initial~~ s^2 ~~(VVM)~~	Max allowable daily rate of change (LL)
Parameters						
β	Soil Moisture exponent	[ ]	*N*(2, 0.1)	0 – 7	0.003	$1.8\text{x}10^{-3}$
$fcap$	Maximum soil moisture store depth	[mm]	*N*(467, 10)	10 – 2000	0.003	0.4
$hl1$	Threshold for generation of near surface flow	[mm]	*N*(120, 10)	0 – 400	0.003	0.1
$K0$	Near Surface Flow Routing Coefficient	[ ]	*N*(0.3, 0.005)	0.0625 – 1	0.003	$2\text{x}10^{-4}$
$K1$	Interflow Routing Coefficient	[ ]	*N*(0.09, $5\text{x}10^{-4}$)	0.02 – 0.1	0.003	$9\text{x}10^{-6}$
$perc$	Percolation rate	[mm/d]	*N*(1.3, 10^{-4})	0 – 3	0.003	10^{-3}
$K2$	Baseflow Routing Coefficient	[ ]	*N*(0.01, 10^{-6})	$5\text{x}10^{-5}$– 0.02	0.003	$9\text{x}10^{-6}$
States						
$sowat$	Soil Moisture Store	[mm]	*N*(0,1)	(0, $fcap$)		
$stw1$	Shallow Layer Store	[mm]	*N*(0,1)	(0, ∞)		
$stw2$	Deep Layer Store	[mm]	*N*(0,0.1)	(0, ∞)		

728 **Table 4 Locally Linear EnKF inputs for the HBV model case**

729

730

Parameters						
	Description	**Units**	**Initial Sampling Distribution**	**Feasible Range**	~~**Initial** s^2 **(VVM)**~~	**Max allowable daily rate of change (LL)**
b	Pareto-distributed soil storage shape parameter	[ ]	$N(0.37, 10^{-4})$	0 – 0.3	0.004	$3x10^{-4}$
c_{max}	Maximum point soil storage depth	[mm]	$N(651, 10)$	300 – 1500	0.004	0.3
k_s	Surface Runoff Routing Coefficient	[ ]	$N(0.6, 5x10^{-4})$	0.55 – 0.99	0.018	$3x10^{-4}$
k_b	Groundwater Routing Coefficient	[ ]	$N(0.04, 5x10^{-4})$	0.001 – 0.54	0.018	$4x10^{-5}$
α	Excess Runoff Splitting Parameter	[ ]	$N(0.47, 5x10^{-4})$	0.001 – 0.99	0.018	$4x10^{-4}$
States						
S	Soil Store	[mm]	$N(180, 0.1*180)$	$(0, S_{max} = \frac{bc_{min}+c_{max}}{b+1})$		
$S_{q1,2,3}$	Quick Flow Stores	[mm]	$N(0,1)$	$(0, \infty)$		
S_s	Slow Flow Store	[mm]	$N(0,1)$	$(0, \infty)$		

Table 5 Locally Linear EnKF inputs for the HYMOD model case

Figures

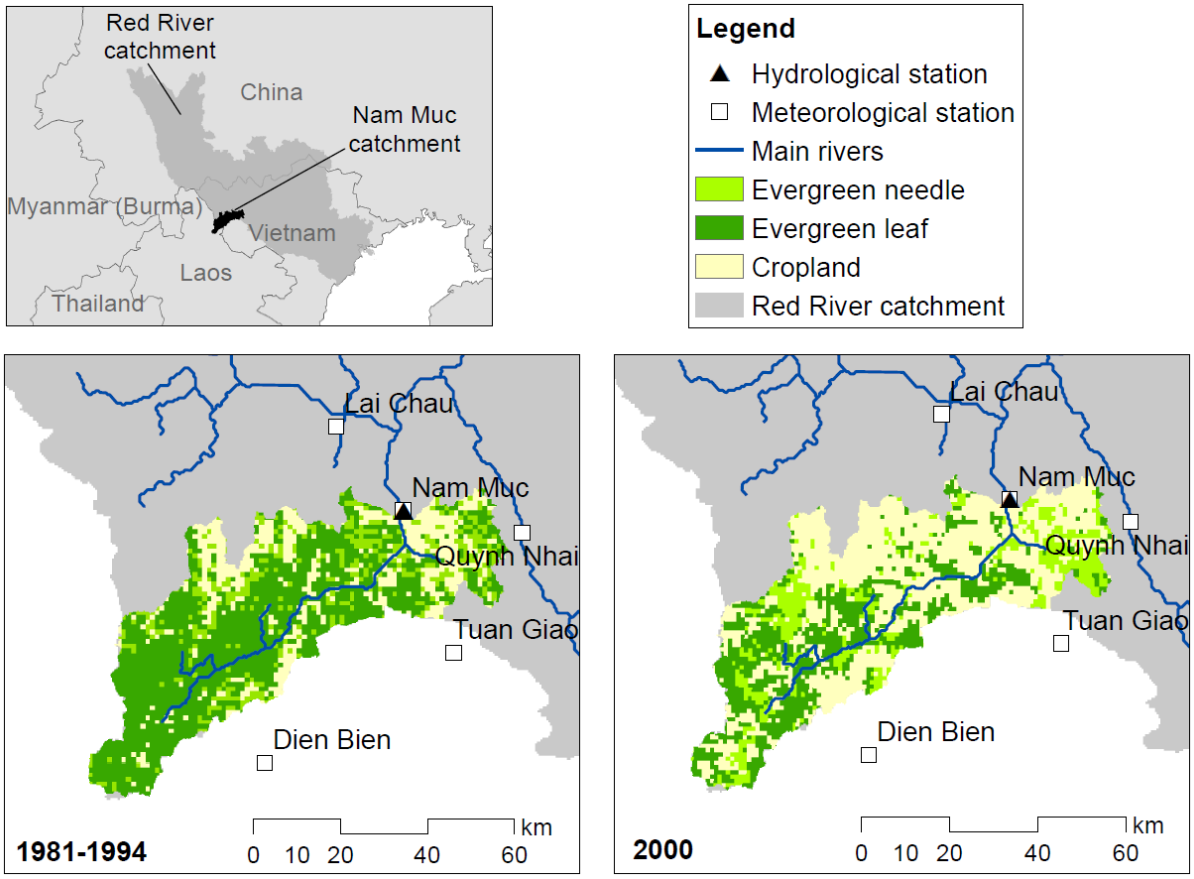

Figure 1 Study Catchment showing gauges and changes in land cover over time.

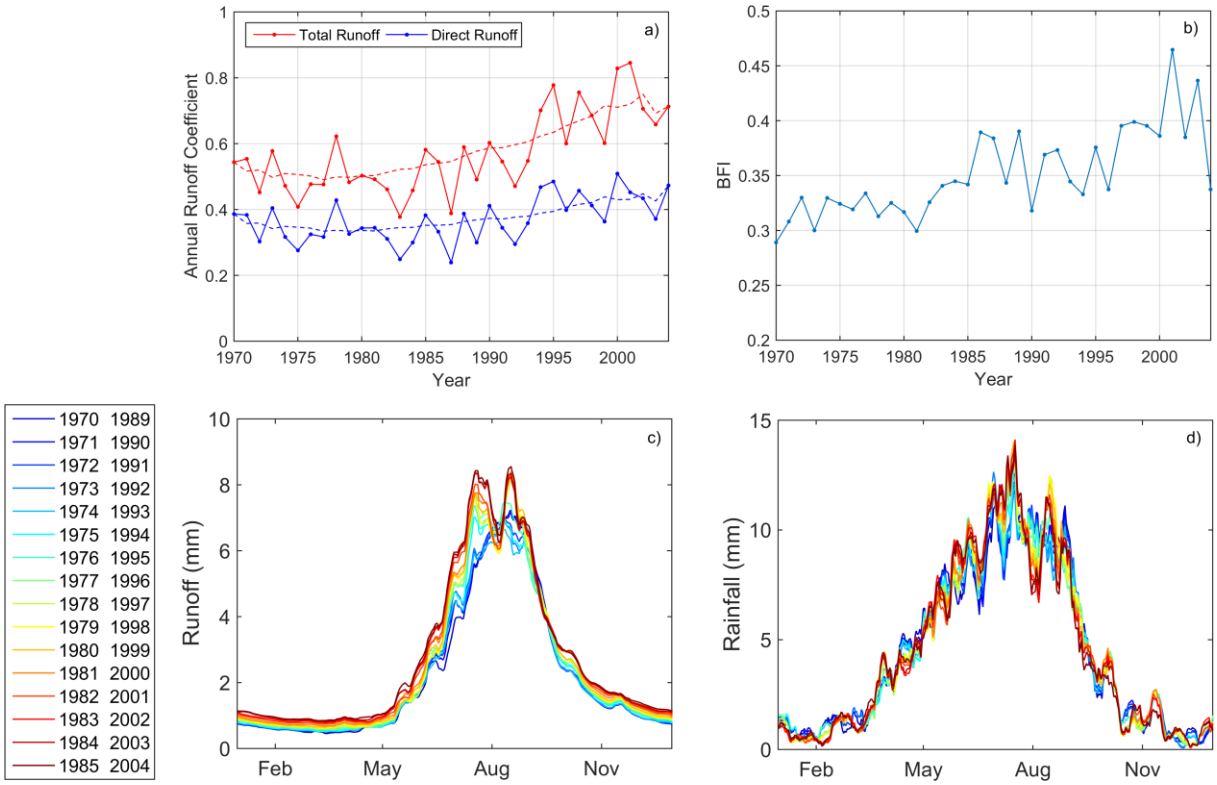

Figure 2 Impact of land use change on observed streamflow: a) Annual Runoff Coefficient, b) Annual Baseflow Index (BFI), c) Moving Average Shifting Horizon (MASH) results for total observed runoff, d) MASH for observed rainfall.

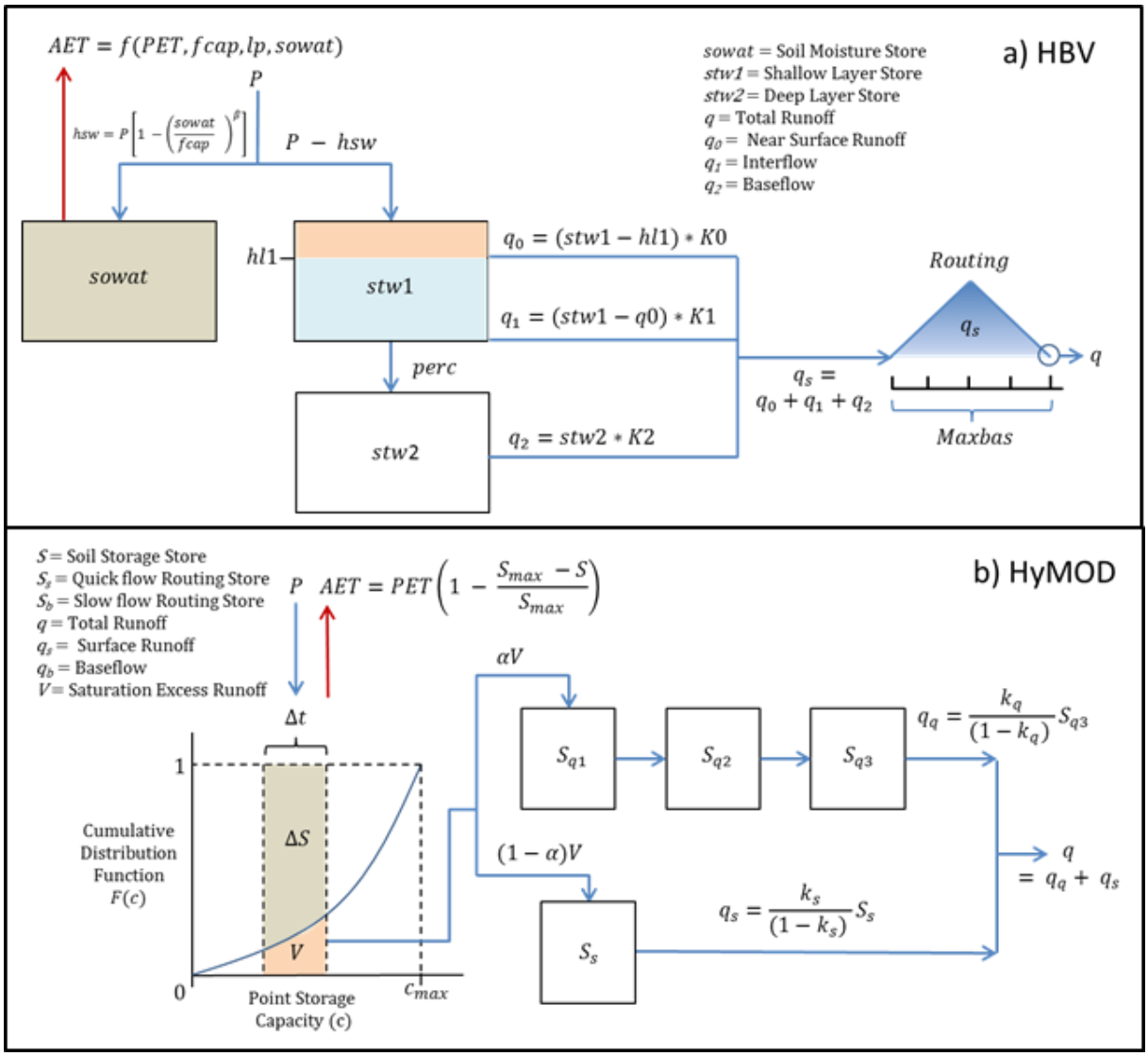

Figure 3 Schematic of the models used in this study: a) HBV and b) HyMOD

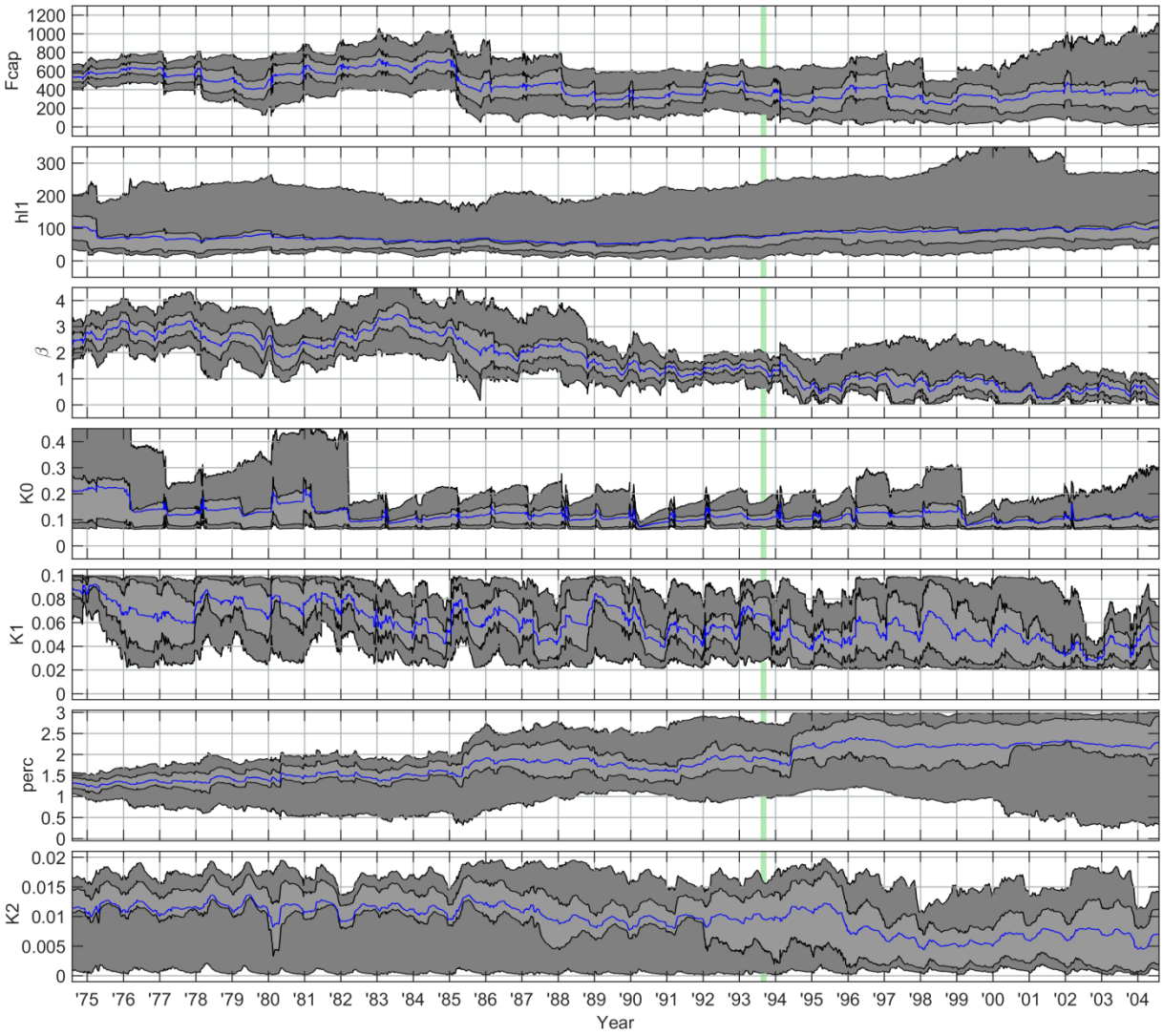

Figure 4 Parameter Trajectories using the HBV model. The dark grey shaded areas indicate the middle 90% of the ensemble, bounded by the 5th and 95th percentiles. The light grey shaded areas indicate the middle 50% of the ensemble, bounded by the 25th and 75th percentiles. The ensemble mean is indicated by the blue line. The vertical green panel indicates the assumed time period of rapid deforestation.

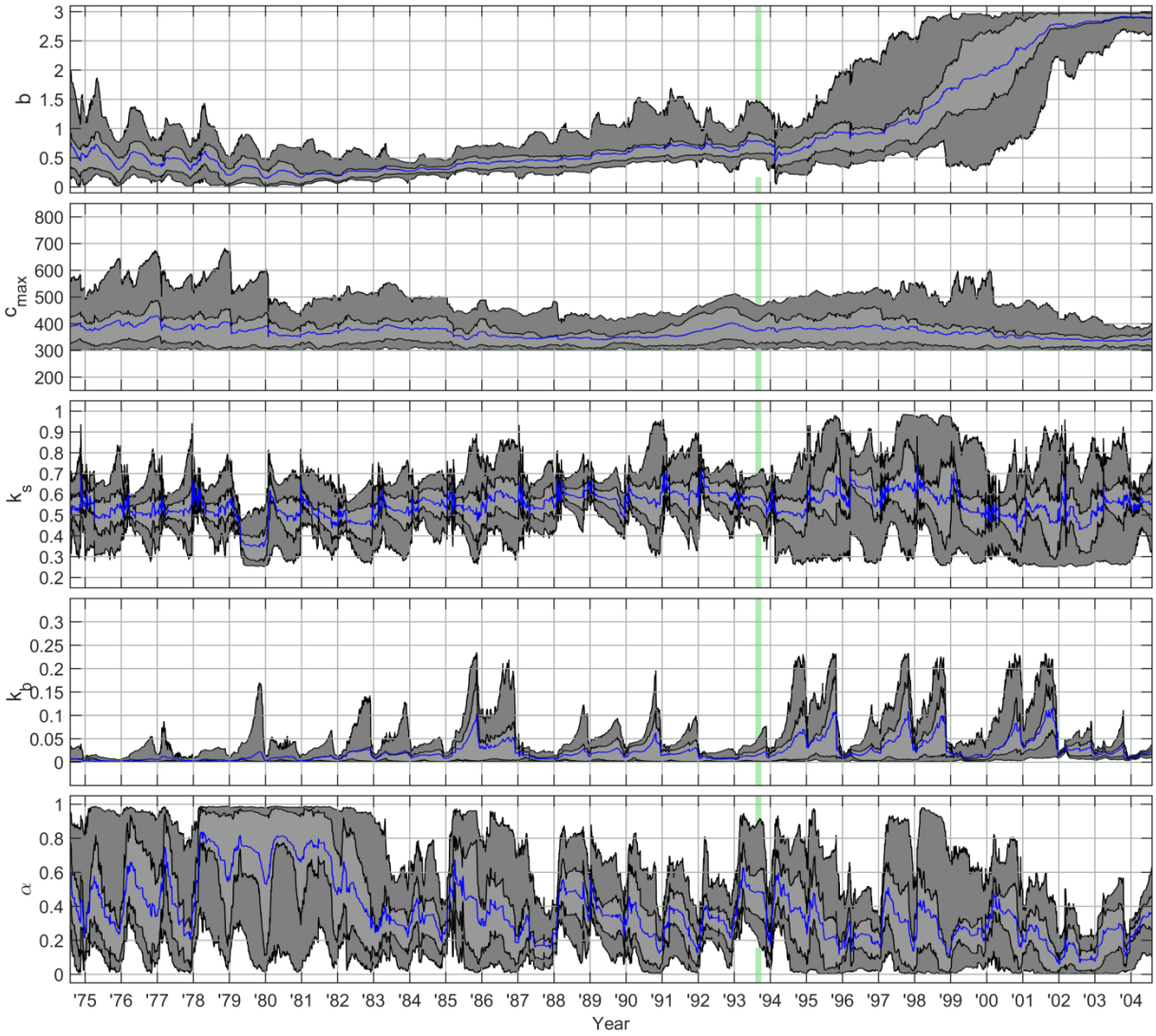

Figure 5 Parameter Trajectories using the HyMOD model. The dark grey shaded areas indicate the middle 90% of the ensemble, bounded by the 5th and 95th percentiles. The light grey shaded areas indicate the middle 50% of the ensemble, bounded by the 25th and 75th percentiles. The ensemble mean is indicated by the blue line. The vertical green panel indicates the assumed time period of rapid deforestation.

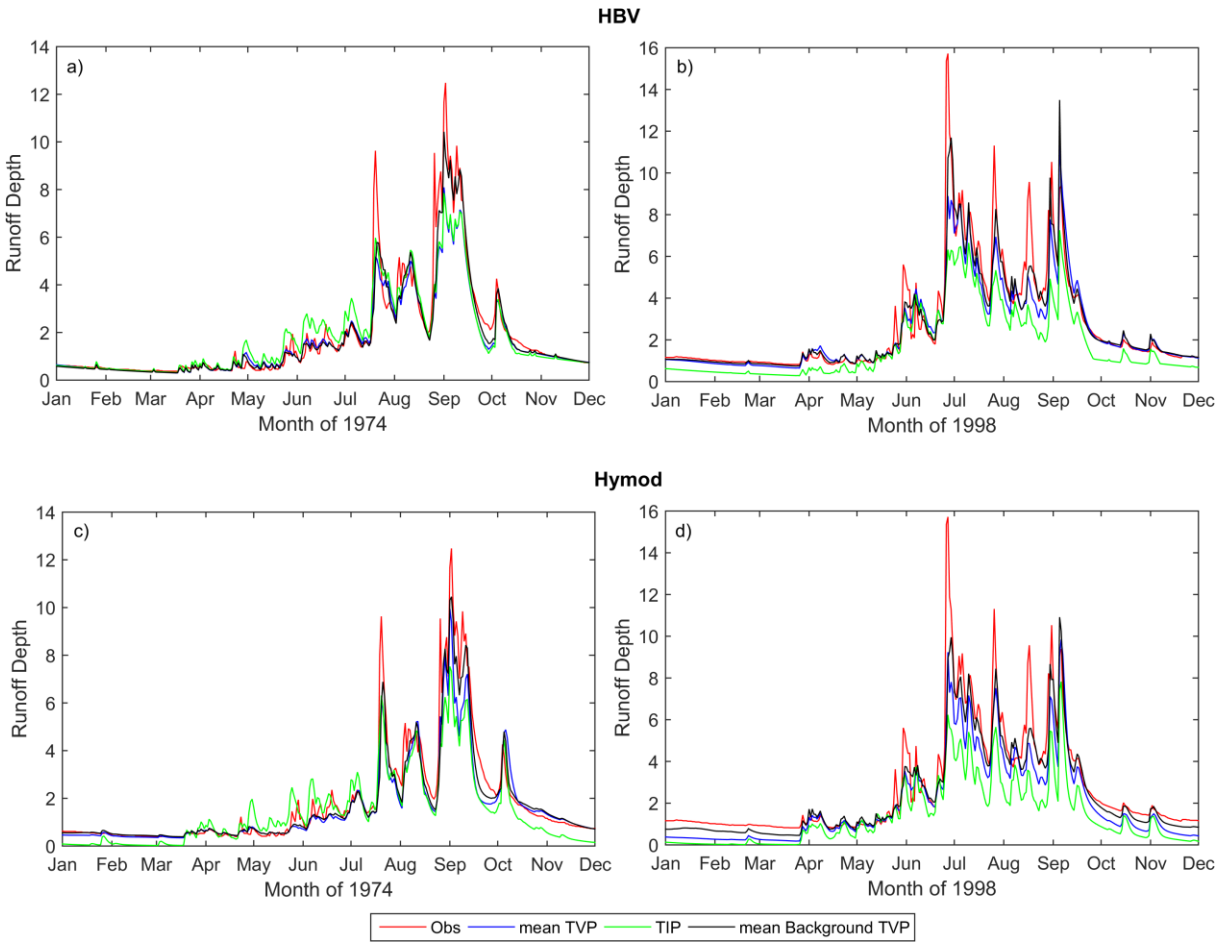

797

798 **Figure 6 Representative Hydrographs of background streamflow from the LL Dual EnKF (black line),**
799 **Time varying parameter model with no state updating (blue line), time invariant parameter model**
800 **with no DA (green line) and observed streamflow (red line). Results for HBV are shown in the top**
801 **row and HyMOD in the bottom row. A pre-change year (1974) is shown on the left and a post**
802 **change year (1998) on the right.**

803
804

805

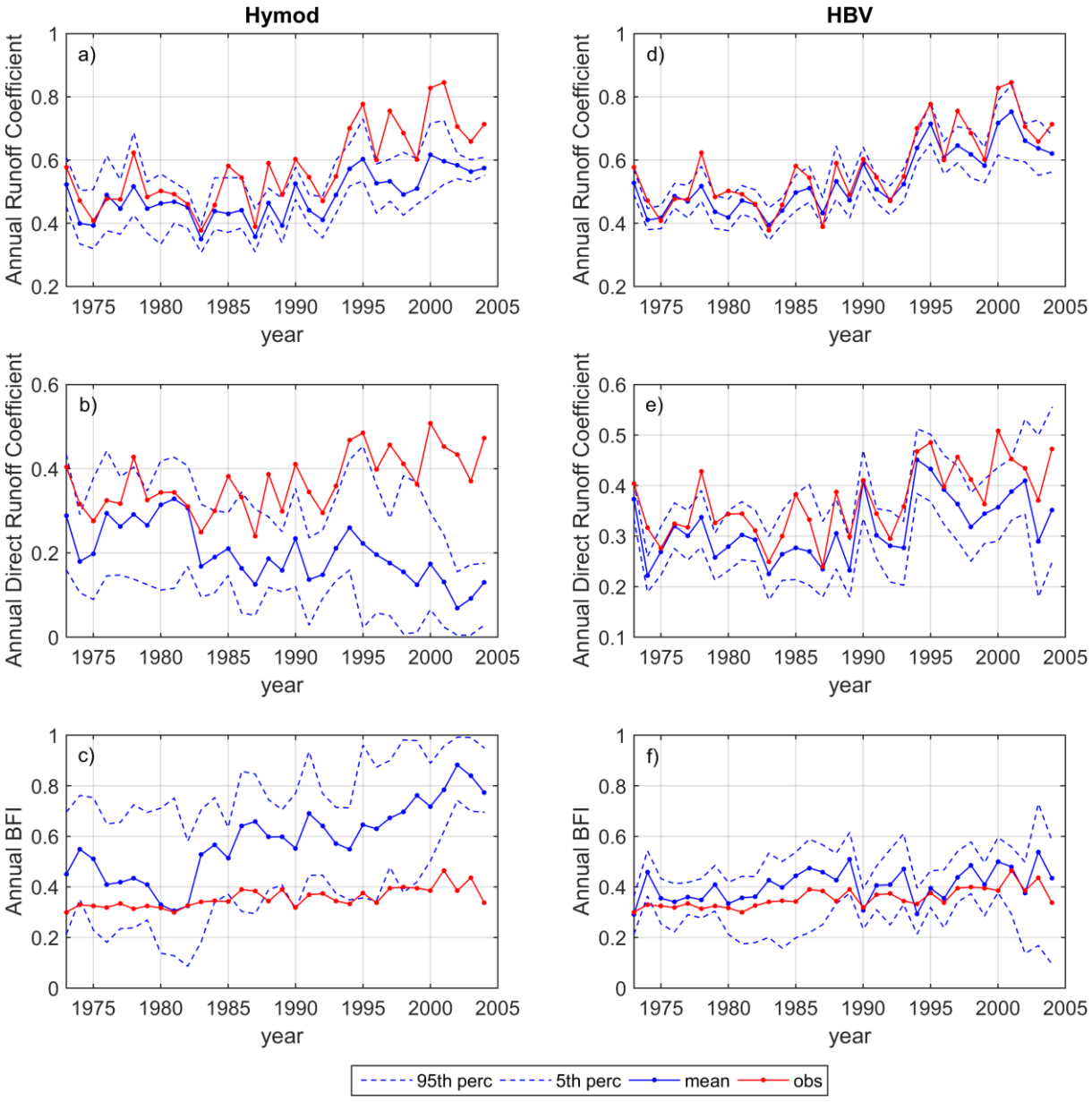

Figure 7 Influence of time varying parameters on model output (i.e. without state updating) summarized in terms of the Annual Runoff Coefficient (top row), Annual Direct Runoff Coefficient (second row) and Annual Baseflow Index (BFI) (third row). Results for HyMOD are shown in the first column, HBV are shown in the second column.

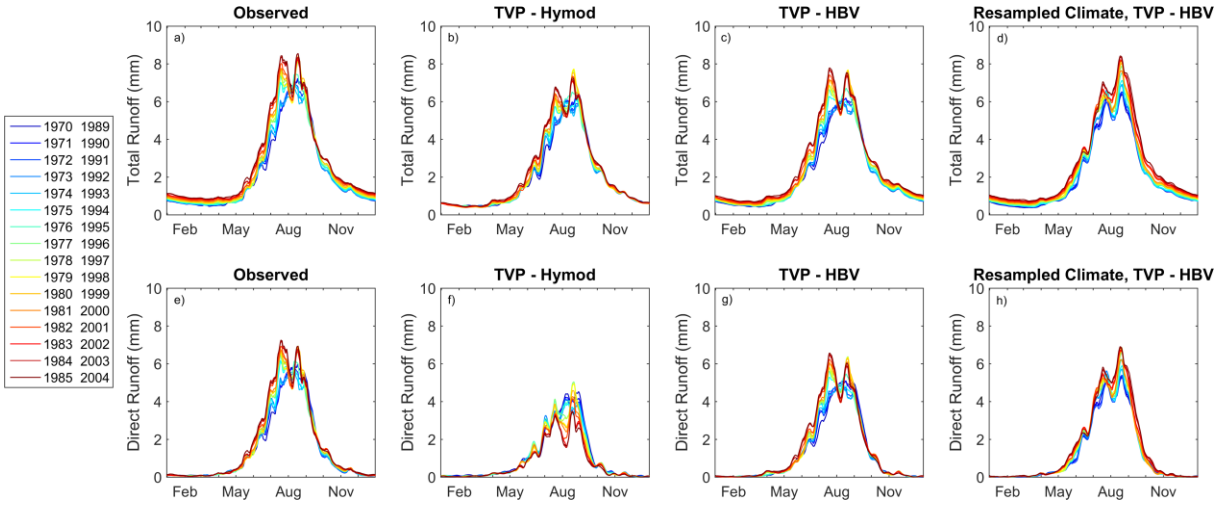

Figure 8 Moving Average Shifting Horizon (MASH) results for observed streamflow (first column), simulated streamflow from time varying parameter model (without state DA) for HYMOD (2nd column), HBV (third column), resampled climate HBV (fourth column). These are split into total runoff (first row) and direct runoff or surface runoff (2nd row).